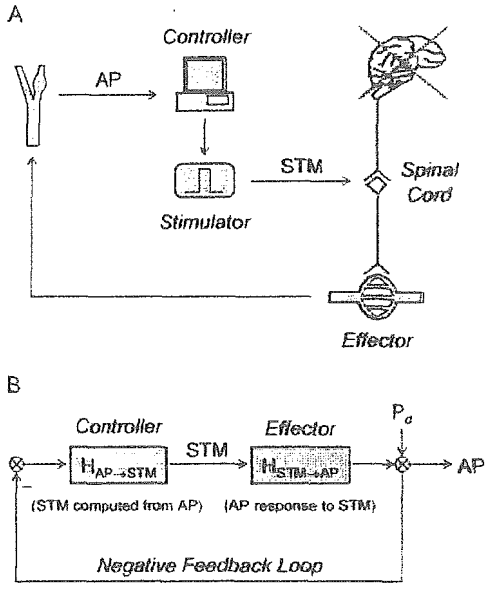

Figure 1. Schematic illustration (A) and block diagram (B) of a BBS. In the context of central baroreflex failure, the BBS automatically computes the frequency (STM) of a pulse train to stimulate sympathetic nerves through an epidural catheter placed at the level of lower thoracic spinal cord, while simultaneously sensing the change in AP. $H_{AP\rightarrow STM}$ denotes a transfer function for the controller functioning as an artificial vasomotor center. $H_{STM\rightarrow AP}$ is a transfer function showing the dynamic response of AP to STM. The overall transfer function of the BBS is given by $H_{AP\rightarrow STM}\times H_{STM\rightarrow AP}$. Therefore, the effect of an external disturbance (P_d) on AP is attenuated to $1/(1+H_{AP\rightarrow STM}\times H_{STM\rightarrow AP})$.

cutes real-time operations that determine the frequency of electrical stimulation (STM) required to minimize the effect of an external disturbance (P_d) on AP and then commands an electrical stimulator to deliver a stimulus of the same frequency to the vasomotor sympathetic nerves via epidural-catheter electrodes placed at the lower thoracic level of the spinal cord. The lower thoracic level was selected as the site for the neural interface of the BBS because the abdominal splanchnic vascular bed is a major effector mechanism for the arterial baroreflex.[23–25]

According to a classic feedback-control theory, ie, feedback correction with proportional and integral gain factors,[26,27] the following algorithm was used to program the controller for the calculation of STM in the frequency domain:

$$(1)\qquad H_{AP\rightarrow STM}=K_p+\frac{K_i}{2\pi fj}$$

where $H_{AP\rightarrow STM}$ is a transfer function from AP to STM, K_p is the proportional correction factor, K_i is the integral correction factor, and j is the imaginary unit. The proportional factor determines the feedback amplification based on the absolute value of the instantaneous control error due to P_d, and the integral factor adjusts the feedback amplification based on the cumulative value of the instantaneous control error. Therefore, STM is computed as follows:

$$(2)\qquad STM=-AP\cdot H_{AP\rightarrow STM}$$

and AP is also expressed as follows:

$$(3)\qquad AP=STM\cdot H_{STM\rightarrow AP}+P_d$$

where $H_{STM\rightarrow AP}$ denotes the frequency response of AP to STM. From Equations 2 and 3, the effect of P_d on AP is estimated as follows:

$$(4)\qquad AP=\frac{1}{1+H_{AP\rightarrow STM}\cdot H_{STM\rightarrow AP}}P_d$$

Thus, if $H_{AP\rightarrow STM}\cdot H_{STM\rightarrow AP}$ is far larger than unity, the BBS can nullify the effect of P_d on AP.

Subjects and Experimental Protocols

A total of 33 patients (46 to 84 years old, 19 males) who underwent orthopedic operations were enrolled in the present study. Ten patients had hypertension, and 4 had diabetes mellitus. None of the subjects had frequent ectopic beats or atrial fibrillation. After induction anesthesia with propofol, an endotracheal tube was introduced orally. The patients were mechanically ventilated with 67% nitrous oxide and 1.5% to 2% end-tidal sevoflurane in oxygen during experimental protocols, while end-tidal carbon dioxide was maintained at 35 to 38 mm Hg. An arterial catheter was placed in the radial artery for AP measurement. To record central venous pressure (CVP), a central venous catheter was placed in the femoral vein, and the tip of the catheter was advanced into the inferior vena cava just above the diaphragmatic level. Furthermore, an epidural catheter was placed percutaneously, and the tip, which contained a pair of electrodes (Unique Medical, Tokyo; interelectrode distance 15 mm), was placed at the level of Th_{9-11}. Placement of the central venous catheter and the epidural catheter was verified by chest radiograph.[28]

Before making an incision of affected areas, we performed 2 different protocols in separate groups of patients. In the first group of patients (n=12, 46 to 76 years old, 7 males) undergoing operations for cervical spondylosis and canal stenosis, the averaged $H_{STM\rightarrow AP}$ was estimated and the $H_{AP\rightarrow STM}$ was designed parametrically with Equation 1 to minimize the effect of P_d on AP. After we programmed the designed $H_{AP\rightarrow STM}$ into the computer, the efficacy of the BBS was tested against the rapid progressive hypotension induced by use of a thigh tourniquet[29–31] in the second group of patients (n=21, 64 to 84 years old, 12 males) undergoing operation for knee joint osteoarthritis. During each protocol, the muscle twitches induced by spinal cord stimulation were prevented by the intravenous administration of vecuronium bromide. Analgesia for the pain provoked by spinal cord stimulation and tourniquet inflation was provided by intravenous injection of fentanyl citrate. In a preliminary study, the validity of the analgesic preparation was confirmed for the experimental protocols, and the safety of spinal cord stimulation for 20 minutes was verified.

Estimation of Transfer Function From STM to AP

To characterize the dynamic nature of the AP response to STM, ie, $H_{STM\rightarrow AP}$, the lower thoracic sympathetic nerves were randomly stimulated for 15 minutes while we recorded AP. According to a white noise method for system identification, the STM was altered between 0 and 20 Hz every 4 seconds. The pulse width of electrical stimuli was fixed at 0.1 ms. The stimulation current was adjusted for each patient so as to produce a pressor response of ≈10 mm Hg at 20 Hz. This resulted in an average current of 15±4 (mean±SD) mA. The electrical signals of STM and AP were digitized at 100 Hz. As described previously,[20–22] the transfer function from STM to AP, $H_{STM\rightarrow AP}$, was estimated with a fast Fourier transform algorithm. Finally, the average of $H_{STM\rightarrow AP}$ among 12 patients was calculated.

Design of Artificial Vasomotor Center

With substitution of the averaged $H_{STM\rightarrow AP}$ for Equation 4, the instantaneous AP response to P_d was simulated numerically, and a stepwise decline with an amplitude of 20 mm Hg was imposed on the BBS. While the feedback parameters of $H_{AP\rightarrow STM}$, ie, K_p and K_i, were altered, the effect of the parameters on the AP response was investigated. Finally, the parameters that enabled the BBS to quickly and stably minimize the effect of P_d on AP were determined.

Efficacy of BBS in a Clinical Model of Transient Hypotension

The performance of the BBS was evaluated in a clinical model of rapid transient hypotension (n=21). Rapid hypotension was evoked by the sudden deflation of a thigh tourniquet, which is widely used to achieve bloodless dissection during total knee arthroplasty.[29–31] Acute hypotension immediately after tourniquet release is a well-

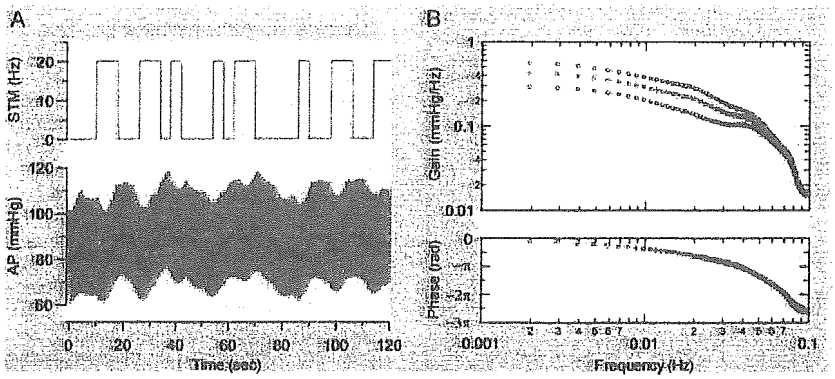

Figure 2. A, Representative example of time series data of the response of AP to random stimulation of the lower thoracic spinal cord. According to quasi-white noise, the STM was randomly altered between 0 and 20 Hz. The AP seems to slowly respond to STM with a delay. B, Transfer function of the AP response to the STM change. Data are expressed as mean±SD for 12 patients. rad indicates radians. See text for explanation.

known phenomenon that results from a rapid decrease in peripheral vascular resistance and an increase in venous pooling in the affected limb.[29] The degree of hypotension can be potentiated by the use of volatile anesthetic agents such as sevoflurane, which are central depressants of arterial baroreflex function.[32,33] Therefore, tourniquet-related hypotension during sevoflurane anesthesia can be used as a model of orthostatic hypotension in central baroreflex failure.

Briefly, a tourniquet was applied to the upper femur and inflated at 300 mm Hg for 60 minutes and then quickly deflated for 10 minutes. The procedure was then repeated. The BBS was activated during 1 of the 2 trials of tourniquet-related hypotension, and the electrical signals of STM, CVP, and AP were digitized at 100 Hz.

Statistical Analysis

The hemodynamic responses to tourniquet release were measured for each subject while the BBS was being activated and inactivated. The effects of the BBS execution on the hemodynamic changes at 10, 50, and 100 seconds after tourniquet release were analyzed by paired *t* tests with Bonferroni adjustment. Differences were considered significant at overall $P<0.05$.

Results

A representative example of original tracings of STM and AP during random stimulation of the spinal cord is shown in Figure 2A. Random on-off change in STM produced a delayed and slow change in AP. The relationship between STM and AP was quantitatively characterized by the frequency domain analysis (Figure 2B). The averaged transfer function from STM to AP, $H_{STM \rightarrow AP}$, had low-pass characteristics with a corner frequency of 0.06 Hz. The gain factor was 0.43 ± 0.13 mm Hg · Hz^{-1} at the steady state (lowest frequency) and gradually decreased with input frequency. The phase spectrum showed that the input-output relationship was in phase and that the phase delay increased toward higher frequencies. The squared coherence, a measure of linear dependence between STM and AP, was >0.9 in the frequency range of interest (data not shown).

The results of simulation for the design of the artificial vasomotor center, $H_{AP \rightarrow STM}$, are presented in Figure 3. The AP responses to the external disturbance P_d were simulated under 12 different combinations with feedback correction factors. Without feedback compensation, ie, when both feedback correction factors were zero, there was no attenuation of the effect of the external disturbance on AP. Therefore, AP fell by 20 mm Hg immediately after the imposition of P_d (Figure 3A, black line). By contrast, if either or both of the correction factors were too large, the underdamped oscillatory response of AP appeared, and the BBS became unstable. On the basis of these results, K_p was set at 1, and K_i was set at 0.1, so that the BBS could quickly and effectively attenuate the effect of the external disturbance (Figure 3B, red line).

A representative example of the results of the performance tests of the BBS is shown in Figure 4A. A sudden

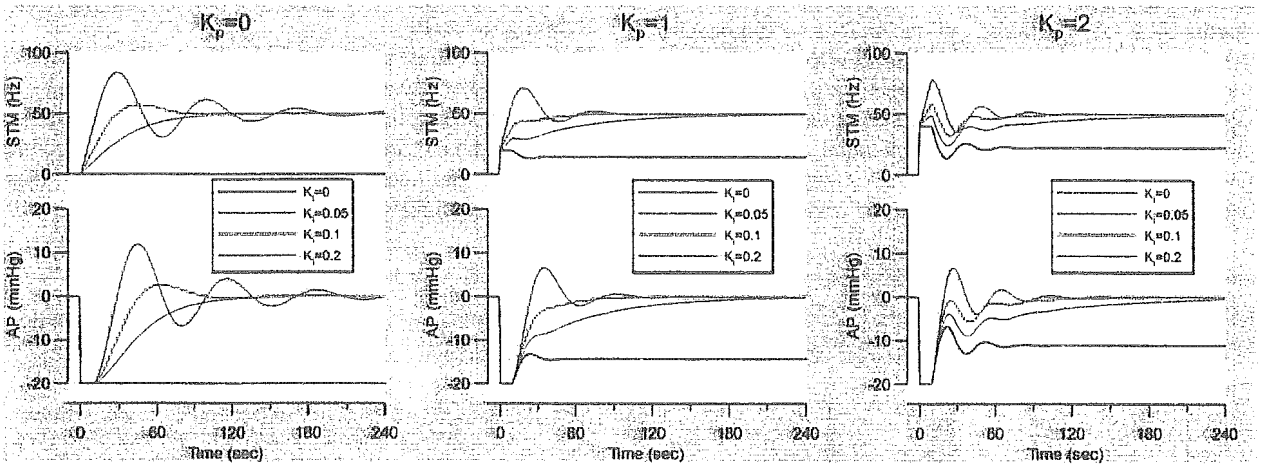

Figure 3. Numerical simulations of a feedback controller of the BBS. A stepwise pressure decline with an amplitude of 20 mm Hg is assumed to be imposed. Results are shown for 12 combinations of proportional (K_p) and integral (K_i) correction factors. See text for explanation.

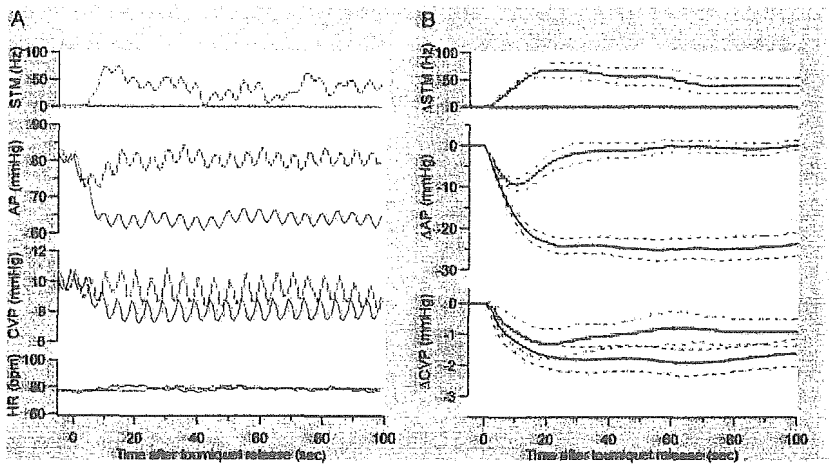

Figure 4. A, Representative example of original tracings of STM, AP, CVP, and heart rate (HR) during 2 episodes of rapid progressive hypotension induced by sudden deflation of a thigh tourniquet in a patient. When the BBS was inactive (blue line), AP decreased immediately after tourniquet release and did not return to baseline level. By contrast, when the BBS was activated (red line), the artificial vasomotor center automatically computed STM and drove an electrical stimulator to restore AP. B, Plots showing averaged changes in STM, AP, and CVP after tourniquet release among 21 patients. Data are expressed as mean (solid line)±SD (dotted line). See text for explanation.

deflation of the thigh tourniquet produced a rapid progressive fall in AP of ≈20 mm Hg within 10 seconds, while lowering CVP by 2 mm Hg. By contrast, when the BBS was activated, STM was computed automatically, and the spinal cord was stimulated appropriately to quickly and effectively attenuate the drop in AP and CVP. Figure 4B summarizes the results obtained from 21 patients, demonstrating effectiveness of the BBS performance in buffering the AP fall in response to the sudden release of the tourniquet. As demonstrated in Figure 5, tourniquet release resulted in an AP decrease of 17±3 mm Hg at 10 seconds, 25±2 mm Hg at 50 seconds, and 24±3 mm Hg at100 seconds. By contrast, during real-time execution of the BBS, the decrease in AP was 9±2 mm Hg at 10 seconds, 1±2 mm Hg at 50 seconds, and 0±1 mm Hg at 100 seconds after the deflation. These data indicated that the BBS significantly attenuated the decrease in AP at these 3 time points and nullified the hypotensive effect of tourniquet release within 50 seconds. Similarly, the BBS significantly suppressed the decrease in CVP within 50 seconds after the release of the tourniquet.

Discussion

Design of BBS

On the basis of knowledge and technology of bionics, we previously developed an artificial feedback control system for automatic regulation of sympathetic vasomotor tone in animal models of central baroreflex failure.[20–22] As a crucial first step to clinical application, we tested its feasibility and efficacy in a clinical model of orthostatic hypotension. A percutaneous epidural catheter approach was established for the monitoring of spinal function during surgery and for pain management,[28] and the lower thoracic level was selected for spinal cord stimulation based on earlier reports that the abdominal splanchnic vascular bed is a major effector mechanism for arterial baroreflex in animals[23,24] and humans.[25] Although the percutaneous epidural approach is less invasive than implantation surgery, spinal cord stimulation excites motor and sensory nerves[12,22,28] in addition to sympathetic vasomotor efferents. Therefore, administration of sufficient doses of muscle relaxants and analgesics was required during experimental protocols. Under these conditions, the dynamic response of AP to STM was easily characterized by the white noise system identification method. Furthermore, the quantitatively estimated results of transfer function analysis (Figure 2B) enabled simulation of the effects of feedback correction factors[27] on performance of the BBS. As demonstrated in Figure 3, the simulation results suggested that the specific combination of feedback correction factors could optimize the performance of the BBS. On the basis of these results, the feedback correction factors were determined to allow the BBS to quickly stabilize AP against the external disturbances.

Efficacy of BBS

The present study utilized a tourniquet-related model of hypotension[29–31] during general anesthesia[32,33] to approximate orthostatic hypotension due to central baroreflex failure. Except for the change in peripheral vascular resistance, the hemodynamic changes after tourniquet deflation are similar to those achieved after upright tilt-

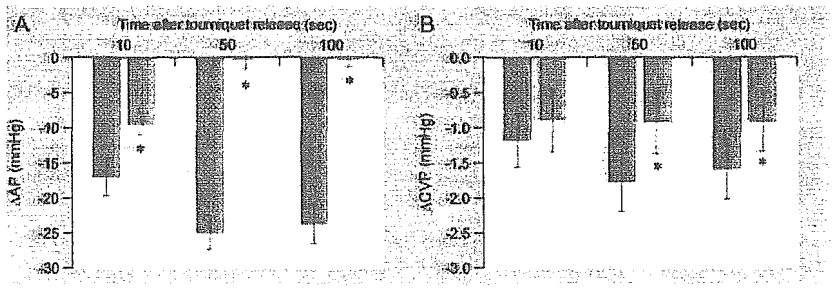

Figure 5. Bar graphs showing changes in AP (A) and CVP (B) at 10, 50, and 100 seconds after tourniquet release. Implementation of the BBS (red column) significantly attenuated tourniquet-related falls (blue column) in AP and CVP. Data are expressed as mean±SD for 21 patients. *Overall $P<0.05$.

ing.[29,31] For example, tourniquet release results in a rapid increase in venous pooling in the affected limb with a subsequent decrease in venous return and cardiac output. Under general anesthesia with volatile gases such as sevoflurane,[32,33] arterial baroreflex function is inhibited, and the hemodynamic disturbance produced by the tourniquet inevitably results in abrupt hypotension. In rare instances, tourniquet deflation can also trigger fatal circulatory collapse.[29]

Despite the fact that the BBS was implemented with fixed values of feedback correction factors for all patients, the BBS successfully stabilized AP against the hemodynamic challenge induced by sudden tourniquet release (Figure 4). These data indicate that the BBS may compensate for some individual differences in the dynamic response of AP to STM.

Finally, the CVP response to STM (Figure 4) in the present study suggests that the BBS attenuated a decrease in venous return. Previous studies have demonstrated that the baroreflex-mediated vasoconstriction in the splanchnic vascular bed is a major mechanism for recruitment of venous return during head-up tilting.[23,25] Therefore, the BBS may functionally mimic the baroreflex control of venous return and control of AP.

Study Limitations

This study possessed several limitations. First, based on the previous results[20–22] obtained from animal studies, the stimulation electrodes were placed in the epidural space at the level of the lower thoracic cord; however, further study to determine the optimal site of electrode placement would be of benefit. Second, it is unclear whether or not the feedback controller designed in the present study is universally applicable to other cases. Although preset parameters for feedback correction were used in the present study, other approaches based on a robust control theory could yield a better result. Finally, the epidural catheter method for sympathetic nerve stimulation is associated with significant pain and discomfort. Thus, practical use of the BBS requires an appropriate method for stimulating only efferent sympathetic nerves.

Clinical Implications

The present study confirmed the efficacy of the BBS in a clinical setting and suggests that the BBS has tremendous potential as a new therapeutic modality for treatment of severe orthostatic intolerance in patients with various syndromes of central baroreflex failure, including Shy-Drager syndrome, baroreceptor deafferentation, and traumatic spinal cord injuries.

Acknowledgments

This study was supported by a Health and Labor Sciences research grant (H14-NANO-002, H16-NANO-005, H15-KOKORO-019) from the Ministry of Health, Labor, and Welfare of Japan and by a grant-in-aid for scientific research (15300165) from the Ministry of Education, Science, Sports, and Culture of Japan.

Disclosures

None.

References

1. Guyton AC, Coleman TG, Granger HJ. Circulation: overall regulation. *Ann Rev Physiol.* 1972;34:13–46.
2. Robertson D. Diagnosis and management of baroreflex failure. *Primary Cardiol.* 1995;21:37–40.
3. Sunagawa K, Sato T, Kawada T. Integrative sympathetic baroreflex regulation of arterial pressure. *Ann N Y Acad Sci.* 2001;940:314–323.
4. Ketch T, Biaggioni I, Robertson R, Robertson D. Four faces of baroreflex failure: hypertensive crisis, volatile hypertension, orthostatic tachycardia, and malignant vagotonia. *Circulation.* 2002;105:2518–2523.
5. Sato T, Kawada T, Inagaki M, Shishido T, Takaki H, Sugimachi M, Sunagawa K. New analytical framework for understanding the sympathetic baroreflex control of arterial pressure. *Am J Physiol Heart Circ Physiol.* 1999;276:H2251–H2261.
6. Shy M, Drager GA. A neurological syndrome associated with orthostatic hypotension: a clinico-pathologic study. *Arch Neurol.* 1960;3:511–527.
7. The Consensus Committee of the American Autonomic Society and the American Academy of Neurology. Consensus statement on the definition of orthostatic hypotension, pure autonomic failure, and multiple system atrophy. *Neurology.* 1996;46:1470.
8. Schatz IJ. Farewell to the "Shy-Drager syndrome." *Ann Intern Med.* 1996;125:74–75.
9. Goldstein DS, Holmes C, Cannon RO III, Eisenhofer G, Kopin IJ. Sympathetic cardioneuropathy in dysautonomias. *N Engl J Med.* 1997;336:696–702.
10. Onrot J, Wiley RG, Fogo A, Biaggioni I, Robertson D, Hollister AS. Neck tumour with syncope due to paroxysmal sympathetic withdrawal. *J Neurol Neurosurg Psychiatry.* 1987;50:1063–1066.
11. Lee HT, Brown J, Fee WE Jr. Baroreflex dysfunction after nasopharyngectomy and bilateral carotid isolation. *Arch Otolaryngol Head Neck Surg.* 1997;123:434–437.
12. Frankel HL, Mathias CJ. Severe hypertension in patients with high spinal cord lesions undergoing electro-ejaculation: management with prostaglandin E_2. *Paraplegia.* 1980;18:293–299.
13. Matthews JM, Wheeler GD, Burnham RS, Malone LA, Steadward RD. The effects of surface anaesthesia on the autonomic dysreflexia response during functional electrical stimulation. *Spinal Cord.* 1997;35:647–651.
14. Wilcox CS, Puritz R, Lightman SL, Bannister R, Aminoff MJ. Plasma volume regulation in patients with progressive autonomic failure during changes in salt intake or posture. *J Lab Clin Med.* 1984;104:331–339.
15. Jordan J, Shannon JR, Diedrich A, Black B, Robertson D, Biaggioni I. Water potentiates the pressor effect of ephedra alkaloids. *Circulation.* 2004;109:1823–1825.
16. Kristinsson A. Programmed atrial pacing for orthostatic hypotension. *Acta Med Scand.* 1983;214:79–83.
17. Bannister R, da Costa DF, Hendry WG, Jacobs J, Mathias CJ. Atrial demand pacing to protect against vagal overactivity in sympathetic autonomic neuropathy. *Brain.* 1986;109:345–356.
18. Kachi T, Iwase S, Mano T, Saito M, Kunimoto M, Sobue I. Effect of L-threo-3,4-dihydroxyphenylserine on muscle sympathetic nerve activities in Shy-Drager syndrome. *Neurology.* 1988;38:1091–1094.
19. Obara A, Yamashita H, Onodera S, Yahara O, Honda H, Hasebe N. Effect of xamoterol in Shy-Drager syndrome. *Circulation.* 1992;85:606–611.
20. Sato T, Kawada T, Shishido T, Sugimachi M, Alexander J Jr, Sunagawa K. Novel therapeutic strategy against central baroreflex failure: a bionic baroreflex system. *Circulation.* 1999;100:299–304.
21. Sato T, Kawada T, Sugimachi M, Sunagawa K. Bionic technology revitalizes native baroreflex function in rats with baroreflex failure. *Circulation.* 2002;106:730–734.
22. Yanagiya Y, Sato T, Kawada T, Inagaki M, Tatewaki T, Zheng C, Kamiya A, Takaki H, Sugimachi M, Sunagawa K. Bionic epidural stimulation restores arterial pressure regulation during orthostasis. *J Appl Physiol.* 2004;97:984–990.
23. Hainsworth R, Karim F. Responses of abdominal vascular capacitance in the anaesthetized dog to changes in carotid sinus pressure. *J Physiol Lond.* 1976;262:659–677.

24. Carneiro JJ, Donald DE. Blood reservoir function of dog spleen, liver, and intestine. *Am J Physiol Heart Circ Physiol.* 1977;232:H67–H72.
25. Minson CT, Wladkowski SL, Pawelczyk JA, Kenney WL. Age, splanchnic vasoconstriction, and heat stress during tilting. *Am J Physiol Regul Integr Comp Physiol.* 1999;276:R203–R212.
26. Marmarelis PZ, Marmarelis VZ. *Analysis of Physiological Systems: The White-Noise Approach.* New York, NY: Plenum; 1978.
27. Kawada T, Sunagawa G, Takaki H, Shishido T, Miyano H, Miyashita H, Sato T, Sugimachi M, Sunagawa K. Development of a servo-controller of heart rate using treadmill. *Jpn Circ J.* 1999;63:945–950.
28. Shimoji K, Hokari T, Kano T, Tomita M, Kimura R, Watanabe S, Endoh H, Fukuda S, Fujiwara N, Aida S. Management of intractable pain with percutaneous epidural spinal cord stimulation: differences in pain-relieving effects among diseases and sites of pain. *Anesth Analg.* 1993;77:110–116.
29. Kahn RL, Marino V, Urquhart B, Sharrock NE. Hemodynamic changes associated with tourniquet use under epidural anesthesia for total knee arthroplasty. *Reg Anesth.* 1992;17:228–232.
30. Feldman DL, Wigod M, Barwick W, Levin LS. Tourniquet-related hypotension in venous stasis ulcer excision. *Ann Plast Surg.* 1993;30: 556–559.
31. Sander-Jensen K, Mehlsen J, Secher NH, Bach FW, Bie P, Giese J, Schwartz TW, Trap-Jensen J, Warberg J. Progressive central hypovolaemia in man–resulting in a vasovagal syncope? Haemodynamic and endocrine variables during venous tourniquets of the thighs. *Clin Physiol.* 1987;7:231–242.
32. Tanaka M, Nishikawa T. Arterial baroreflex function in humans anaesthetized with sevoflurane. *Br J Anaesth.* 1999;82:350–354.
33. Keyl C, Schneider A, Hobbhahn J, Bernardi L. Sinusoidal neck suction for evaluation of baroreflex sensitivity during desflurane and sevoflurane anesthesia. *Anesth Analg.* 2002;95:1629–1636.

CLINICAL PERSPECTIVE

Central baroreflex failure due to Shy-Drager syndrome, baroreceptor deafferentation, and traumatic spinal cord injuries results in severe orthostatic hypotension. However, most commonly used interventions, such as salt loading, cardiac pacing, and pharmacological approaches, can neither restore nor reproduce the functioning of a native vasomotor center. Here, we proposed a novel therapeutic strategy against central baroreflex failure and developed a bionic baroreflex system (BBS). The BBS consisted of a pressure sensor, computer, electrical stimulator, and epidural catheter with sympathetic nerve stimulation electrodes. While automatically calculating the frequency of a pulse train in response to a change in arterial pressure, the computer drove the stimulator at the appropriate frequency to stabilize arterial pressure against an external disturbance. According to a parametric negative-feedback control theory, we designed an algorithm of the computer functioning as an artificial vasomotor center. The efficacy of the BBS was tested in a clinical model of orthostatic hypotension during knee joint surgery. Without the implementation of the BBS, a sudden deflation of a thigh tourniquet resulted in rapid progressive hypotension. By contrast, during real-time execution of the BBS, arterial pressure was quickly restored to the baseline level before tourniquet release. These results suggest the technical feasibility of functional restoration of arterial baroreflex with the BBS.

Efferent Vagal Nerve Stimulation Protects Heart Against Ischemia-Induced Arrhythmias by Preserving Connexin43 Protein

Motonori Ando, PhD; Rajesh G. Katare, MD; Yoshihiko Kakinuma, MD; Dongmei Zhang, MD; Fumiyasu Yamasaki, MD; Kazuyo Muramoto, PhD; Takayuki Sato, MD

Efferent Vagal Nerve Stimulation Protects Heart Against Ischemia-Induced Arrhythmias by Preserving Connexin43 Protein

Motonori Ando, PhD; Rajesh G. Katare, MD; Yoshihiko Kakinuma, MD; Dongmei Zhang, MD; Fumiyasu Yamasaki, MD; Kazuyo Muramoto, PhD; Takayuki Sato, MD

Background—Myocardial ischemia (MI) leads to derangements in cellular electrical stability and the generation of lethal arrhythmias. Vagal nerve stimulation has been postulated to contribute to the antifibrillatory effect. Here, we suggest a novel mechanism for the antiarrhythmogenic properties of vagal stimulation during acute MI.

Methods and Results—Under anesthesia, Wistar rats underwent 30 minutes of left coronary artery (LCA) ligation with vagal stimulation (MI-VS group, n=11) and with sham stimulation (MI-SS group, n=12). Eight of the 12 rats in the MI-SS group had ventricular tachyarrhythmia (VT) during 30-minute LCA ligation; on the other hand, VT occurred in only 1 of the 11 rats in the MI-VS group (67% versus 9%, respectively). Atropine administration abolished the antiarrhythmogenic effect of vagal stimulation. Immunoblotting revealed that the MI-SS group showed a marked reduction in the amount of phosphorylated connexin43 (Cx43), whereas the MI-VS group showed only a slight reduction compared with the sham operation and sham stimulation group (37±20% versus 79±18%). Immunohistochemistry confirmed that the MI-induced loss of Cx43 from intercellular junctions was prevented by vagal stimulation. In addition, studies with rat primary-cultured cardiomyocytes demonstrated that acetylcholine effectively prevented the hypoxia-induced loss of phosphorylated Cx43 and ameliorated the loss of cell-to-cell communication as determined by Lucifer Yellow dye transfer assay, which supports the in vivo results.

Conclusions—Vagal nerve stimulation exerts antiarrhythmogenic effects accompanied by prevention of the loss of phosphorylated Cx43 during acute MI and thus plays a critical role in improving ischemia-induced electrical instability. (*Circulation*. 2005;112:164-170.)

Key Words: arrhythmia ■ connexins ■ electrical stimulation ■ gap junctions ■ vagus nerve

Acute myocardial ischemia results in a dramatic reduction of tissue pH, an increase in interstitial potassium levels, an increase in intracellular calcium concentration, and neurohumoral changes, all of which contribute to the development of electrical instability that leads to life-threatening cardiac arrhythmias.[1,2] In particular, cell-to-cell electrical uncoupling of ventricular myocytes plays an important role in arrhythmogenesis during acute and chronic ischemic heart disease.[3–6]

Gap-junction channels, composed of highly homologous proteins known as connexins in vertebrate species, have been implicated in the electrical coupling of excitable tissues, such as cardiac muscles. There are essentially 2 subtypes of connexins (Cx), Cx40 and Cx43, in the adult heart muscle. Cx43 is predominantly expressed in ventricular tissue, whereas Cx40 is mainly found in atrial tissue and in the conduction system.[7] The protein content of ventricular Cx43 is remarkably reduced in ischemia[8,9] and heart failure.[10,11] Gene-targeting studies demonstrate that reduced expression of Cx43 increases the incidence of ventricular tachyarrhythmias[12] and causes a significant reduction in conduction velocity in mice during acute myocardial ischemia.[13] These results suggest that the dysfunction of Cx43 in cardiomyocytes could be one of the components of the substrate that promotes lethal ventricular tachyarrhythmias.

With regard to life-threatening arrhythmias in acute ischemia, the effect of vagal nerve stimulation (VS) has been reported to prevent ventricular fibrillation in dogs.[14] Recently, VS therapy markedly improved long-term survival in an animal model of chronic heart failure after myocardial infarction,[15] and earlier studies have demonstrated that ventricular arrhythmia is one of the major causes of death in chronic heart failure conditions.[16] However, the mechanisms of VS on myocardial infarction remain unknown. With these in mind, we hypothesized that VS would exert an antiarrhythmogenic effect even in acute myocardial ischemia by target-

Received June 21, 2004; de novo received November 28, 2004; revision received March 25, 2005; accepted March 30, 2005.

From the Department of Cardiovascular Control (M.A., R.G.K., Y.K., D.Z., T.S.), Kochi Medical School, Nankoku, Japan; Department of Clinical Laboratory (F.Y.), Kochi Medical School, Nankoku, Japan; and Department of Integrative Physiology (K.M.), Kochi Medical School, Nankoku, Japan.

Correspondence to Takayuki Sato, Department of Cardiovascular Control, Kochi Medical School, Nankoku, Kochi 783-8505, Japan. E-mail tacsato-kochimed@umin.ac.jp

Circulation is available at http://www.circulationaha.org

DOI: 10.1161/CIRCULATIONAHA.104.525493

ing the gap junctions. Therefore, in the present study, using both an in vivo acute ischemia model in rats and in vitro primary cultured cardiomyocytes from neonatal rats, we examined the effects of VS on arrhythmogenesis during acute myocardial ischemia.

Methods

The care and use of animals were in strict accordance with the guiding principles of the Physiological Society of Japan.

In Vivo Arrhythmia Study

Male Wistar rats (SLC, Japan) weighing 270 to 300 g were assigned to 6 groups receiving the following treatments: sham-operated rats treated with sham stimulation (SO-SS, n=6), sham-operated rats treated with vagal stimulation (SO-VS, n=5), myocardial ischemia rats with sham stimulation (MI-SS, n=12), myocardial ischemia rats with vagal stimulation (MI-VS, n=11), myocardial ischemia rats with both vagal stimulation and atropine administration (MI-VS-Atr, n=6), and myocardial ischemia rats preconditioned by vagal stimulation (pcVS-MI, n=9).

Acute Ischemia Model

After induction of anesthesia, the rat was ventilated artificially with a volume-controlled rodent respirator (model 683, Harvard Apparatus) at 80 strokes per minute. Anesthesia was maintained through the use of 1.2% halothane during surgical procedures and 0.6% halothane during data recording. Left ventricular MI was induced by 30 minutes of left coronary artery (LCA) ligation. In sham-operated rats, we loosely tied a suture around the LCA without arterial occlusion. For measurement of arterial pressure, a polyethylene tubing (PE-10, Becton Dickinson) that was filled with saline and connected to a fluid-filled transducer (DX-300, Viggo-Spectramed) was cannulated into the right femoral artery. Experimental solutions were infused through another polyethylene tubing, which was cannulated into the right femoral vein. Atropine sulfate (1 mg/kg) (Sigma) was administered as vagal efferent muscarinic blockade. For the prevention of dehydration during experiments,[17] physiological saline was continuously infused at a rate of 5 mL · kg^{-1} · h^{-1} with a syringe pump (CFV-3200; Nihon Kohden).

Vagal Nerve Stimulation

The right vagal nerve was identified, isolated, and cut in the neck region. Only the distal end of the vagal nerve was placed on a pair of platinum wires and was used for stimulation to exclude the effects of vagal afferent. The electrode was connected to an isolated constant voltage stimulator (SS-202J and SEN-7203, Nihon Kohden). The vagal nerve was stimulated with electrical rectangular pulses of 0.1-ms duration at 10 Hz during LCA ligation. The electrical voltage of pulses was optimized in each rat to obtain a 10% reduction in heart rate before LCA ligation. The actual electrical voltage was in the range of 2 to 6 V. VS was started at 1 minute before LCA ligation and continued for 30 minutes after LCA ligation. A run of first spontaneous ventricular tachyarrhythmia (VT) was defined as 10 or more beats with a cycle length <100 ms.

To exclude vagally induced bradycardiac effects during MI and to investigate whether or not a heart preconditioned by VS (pcVS) was insusceptible to ischemia-induced VT, we also examined the effect of 10-minute VS only before LCA ligation. After a 5-minute stabilization period for the recovery of heart rate, the rat was subjected to 30-minute LCA ligation.

Risk Area Assessment

To confirm the ischemic area induced by LCA ligation, 2 mL of 2% Evans blue dye was injected via the femoral vein at the end of 30 minutes of coronary artery ligation. The area at risk was determined by negative staining with Evans blue. Area measurements were determined with Image-Pro version 4.0 (Media Cybernetics).

Excised Heart Study

We conducted this protocol separately from the in vivo arrhythmia study because the experimental preparation of Evans blue dye injection for risk area assessment did not allow us to perform immunoblotting and immunohistochemical assay of excised hearts. For each group, we prepared and analyzed 5 hearts.

Protein Preparation and Immunoblotting

Pulverized frozen left ventricle samples were suspended in 40 vol of ice-cold 10% trichloroacetic acid and homogenized with a tissue homogenizer (2 bursts, 30 seconds each).[18] Homogenates were centrifuged at 10 000*g* for 10 minutes. Supernatants were discarded, and the remaining pellets were resuspended in sampling solution (9 mol/L urea, 0.065 mol/L dithiothreitol, 2% Triton X-100) and sonicated. After addition of 0.37 mol/L lithium dodecylsulfate, the protein-containing solution was neutralized by 1 mol/L Tris solution, and sonicated again. For immunoblot analysis, proteins separated by SDS-PAGE with 15% polyacrylamide gels were transferred electrophoretically to polyvinylidene difluoride sheets (Millipore). After 1 hour of blocking in the 4% skimmed milk solution, the membrane was incubated overnight with anti-Cx43 antibody (71-0700, Zymed) diluted 1:1000. Blots were then incubated for 1 hour with horseradish peroxidase–conjugated goat anti-rabbit IgG, developed with an ECL chemiluminescence reagent (Amersham), and exposed to a medical x-ray film. Equal protein content in all the samples was confirmed by Coomassie brilliant blue staining.

Immunohistochemistry and Confocal Microscopy

Transmural blocks of left ventricular myocardium from selected hearts were immersed in a fixative containing 4% paraformaldehyde and 0.1 mol/L phosphate buffer (pH 7.4), embedded in paraffin, and sectioned at a thickness of 4 μm. Sections were deparaffinized, placed in citrate buffer, and boiled in a microwave oven for 10 minutes to enhance specific immunostaining. The sections were then incubated overnight with anti-Cx43 antibody diluted 1:100 and then incubated for 2 hours in Alexa546-conjugated goat anti-rabbit IgG (Molecular Probes) diluted 1:100. Fluorescence of Alexa546 was observed with a confocal laser scanning microscope system (FV300, Olympus). Reconstructed projection images were obtained from serial optical sections recorded at an interval of 0.5 μm.

Primary Culture Study

We used neonatal rat primary cultured cardiomyocytes to investigate the direct action of acetylcholine (ACh), a neurotransmitter released by VS, on phosphorylated Cx43. Hearts were excised from 1- to 2-day-old neonatal Wistar rats and digested with 0.03% type IV collagenase (Sigma) and 0.03% trypsin (Invitrogen). After digestion, cardiomyocytes were washed repeatedly in serum containing culture medium and were preplated for 90 minutes in the noncoated culture dish in the presence of DMEM medium (Sigma) with 10% FBS to remove the contaminating noncardiomyocytes. Next, cardiomyocytes were plated and cultured in gelatin-coated culture dishes in DMEM medium with 10% FBS. New medium was replaced every day, and all experiments were performed after 4 days of culture.

Hypoxia and Immunoblotting

For hypoxia experiments, cardiomyocytes in serum-deficient DMEM were transferred into an airtight incubator and maintained at a humidified hypoxic atmosphere of <2% O_2 with nitrogen and 5% CO_2 for 30 minutes. Cells were treated either with ACh (0.5 mmol/L) alone or with both ACh and atropine (0.1 mmol/L) 10 minutes before the cells were subjected to hypoxia. After 30 minutes, the treated cells were sampled for immunoblotting.

Dye Transfer Assay

To assess the effect of ACh on cell-to-cell communication, we monitored dye transfer in primary cultured cardiomyocytes with Lucifer Yellow CH (LY; lithium salt, Molecular Probes). Cells in the culture medium were viewed on a Zeiss microscope equipped with fluorescence illumination and FITC filters. The emitted fluorescent light was projected onto a CCD camera system (C4742-98-24ER,

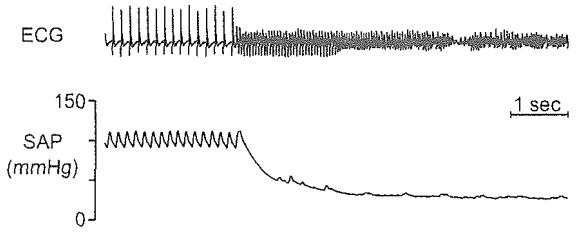

Figure 1. Example of run of VT induced by LCA ligation in rat treated with sham stimulation. In this case, ventricular fibrillation was initiated after ventricular tachycardia. SAP indicates systemic arterial pressure.

Hamamatsu Photonics). LY was injected electrophoretically via a conventional intracellular microelectrode made from borosilicate glass capillaries. The outer diameter of microelectrodes was 0.15 to 0.25 μm, and the tip resistance of these electrodes filled with 3% LY was 0.6 to 1.4 GΩ. An inward square-pulse current (20 to 40 nA) of 0.5-second duration was injected at a frequency of 1 Hz for 2 to 3 minutes using the circuitry of an amplifier (707, WPI) and a voltage pulse generator (SEN7203, Nihon Kohden). For induction of the hypoxic condition, cardiomyocytes were treated for 5 hours with 0.2 mmol/L $CoCl_2$,[19] because microinjection methods are not suitable for gas-tight chamber experiments with N_2 substitution. Cells were treated either with ACh (0.5 mmol/L) alone or with both ACh and atropine (0.1 mmol/L) before chemical hypoxia. Dye injection was performed at room temperature (24°C to 26°C).

Statistical Analysis

Time of onset of the first run of VT was analyzed by the Kaplan-Meier method, and comparisons were made with the Mantel-Haenszel log-rank test. A nonparametric test for comparison of treatments with a control was performed by a Mann-Whitney U test with Bonferroni adjustment. Differences were considered significant at $P<0.05$. Values are expressed as mean±SD.

Results

In Vivo Arrhythmia Study

Effects of VS on Acute Ischemia-Induced VT

Figure 1 illustrates an example of the VT observed after LCA ligation with sham stimulation in the MI-SS group. As demonstrated in this case, VT followed by ventricular fibrillation was often detected after LCA ligation without VS. Figure 2 shows the time of onset and the incidence of the first spontaneous VT after LCA ligation. Eight of 12 rats in the MI-SS group experienced VT; on the other hand, only 1 of 11 in the MI-VS group developed VT during the 30-minute LCA ligation (67% versus 9%, $P=0.005$). VS achieved an 87% reduction in the relative incidence ratio of VT. In all cases, the first runs of VT were observed within 15 minutes after LCA ligation. Atropine administration abolished the anti-VT effects of VS; 4 of 6 rats developed VT (Figure 2). No VT was detected in either the SO-SS or SO-VS groups.

To exclude vagally induced bradycardiac effects on the incidence of VT, a group of 9 rats were subjected to preconditioning by VS (pcVS-MI group; see Methods). There was no significant difference in heart rate between the MI-SS and pcVS-MI groups immediately before and after LCA ligation (Table). Nevertheless, only 2 of 9 rats in the pcVS-MI group developed VT (22%, $P=0.04$ versus the MI-SS group).

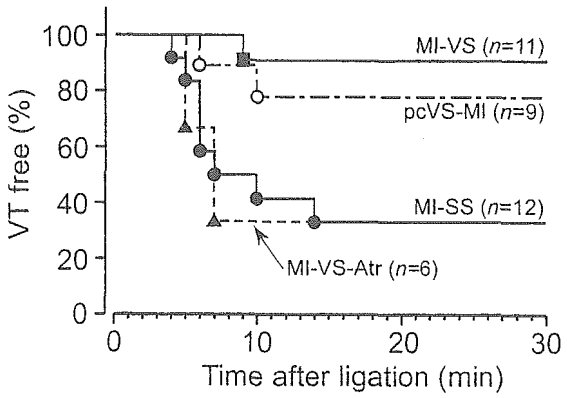

Figure 2. Incidence and onset of first VT after LCA ligation. Myocardial ischemia rats treated with sham stimulation (MI-SS, ●, n=12) and with vagal stimulation (MI-VS, ■, n=11). VS significantly ($P=0.005$ vs MI-SS group) decreased incidence of ischemia-induced VT. In contrast, atropine administration blocked antiarrhythmogenic effect by VS during acute MI (MI-VS-Atr, ▲, n=6). Preconditioning by VS significantly ($P=0.04$ vs MI-SS group) decreased incidence of ischemia-induced VT (pcVS-MI, ○, n=9).

Risk Area Assessment and Hemodynamic Parameters

There was no significant difference in risk area between the MI-SS and MI-VS groups (55±6% versus 59±3%). The differences in heart rate between groups with or without VS reached ≈50 bpm, and after 30-minute ischemia, only the MI-VS group had a significantly lower arterial pressure than the SO-SS group (Table).

Excised Heart Study

Effects of VS on Cx43 Expression

The polyclonal anti-Cx43 antibody in the present study showed closely spaced bands migrating between 43 and 46 kDa and a faint band migrating at 41 kDa. Previous reports[20] demonstrated that the higher- and lower-molecular-weight bands represent phosphorylated and nonphosphorylated isoforms of Cx43, respectively. Figure 3A shows a representative immunoblot prepared with anti-Cx43 antibody. The phosphorylated isoform of Cx43 (bands with 43 kDa) in the MI-VS group was preserved compared with that in the MI-SS group. Quantitative densitometric analysis revealed the level of the phosphorylated isoform of Cx43 in the MI-VS group was maintained at 79±18% of that in the SO-SS group; on the other hand, the level of phosphorylated Cx43 in the MI-SS group was reduced significantly to 37±20% of that in the SO-SS group (Figure 3B). The phosphorylated Cx43 in the SO-VS group was increased significantly to 120±8% of that in the SO-SS group. Atropine inhibited the preserving effects of VS on Cx43 in the MI-VS-Atr group (47±12%). In addition, protein analysis also confirmed that the phosphorylated Cx43 in the pcVS -MI group was at almost the same level as in the SO-SS group (97±20%).

Effects of VS on Cx43 Localization

To investigate the distribution of Cx43 during acute ischemia with or without VS, we performed confocal image analysis of left ventricular tissues stained with anti-Cx43 antibody. As shown in Figure 4A, localization of immunoreactive signals

Heart Rate and Mean Arterial Pressure Immediately Before and After 30-Minute LCA Ligation

		Heart Rate, bpm		Mean Arterial Pressure, mm Hg	
Group	n	Before	After 30-Minute Ligation	Before	After 30-Minute Ligation
SO-SS	6	404±24	414±24	118±14	116±13
SO-VS	5	362±10*	348±15*	106±9	96±6
MI-SS	12	395±22	365±43	117±7	102±10
MI-VS	11	354±12*	353±31*	102±13	90±6*
MI-VS-Atr	6	409±20	362±48	103±8	94±15
pcVS-MI	9	391±33	372±36	109±11	103±10

VS was started at 1 minute before LCA ligation and continued for 30 minutes after LCA ligation. pcVS was performed during 10 minutes without LCA ligation, and after a 5-minute stabilization period for recovery of heart rate, rats were subjected to a 30-minute LCA ligation. Values are mean±SD immediately before and after 30-minute LCA ligation.

*$P<0.05$ vs SO-SS group.

in the SO-SS group was restricted to intercellular junctions, consistent with the gap junctions and intercalated disks. In contrast, the Cx43 signal was reduced dramatically in the MI-SS group (Figure 4B); however, the Cx43 signal in the MI-VS group was almost comparable to the level in the SO-SS group (Figure 4C). These observations indicate that the loss of phosphorylated Cx43 during acute ischemia was prevented by VS.

Primary Culture Study

Effects of Hypoxia and ACh on Cx43 Expression

To examine the muscarinic effect on hypoxia-induced loss of phosphorylated Cx43, immunoblot analysis was performed in primary cultured cardiomyocytes. Under normoxic conditions, addition of ACh for 30 minutes significantly increased the phosphorylated isoform of Cx43 compared with the control group (Figure 5). Although hypoxia for 30 minutes decreased phosphorylated Cx43, ACh treatment prevented this hypoxia-induced loss of Cx43. Atropine inhibited the preserving effects of ACh. Thus, these results indicate that ACh preserved phosphorylated Cx43 through a muscarinic receptor during 30-minute hypoxia.

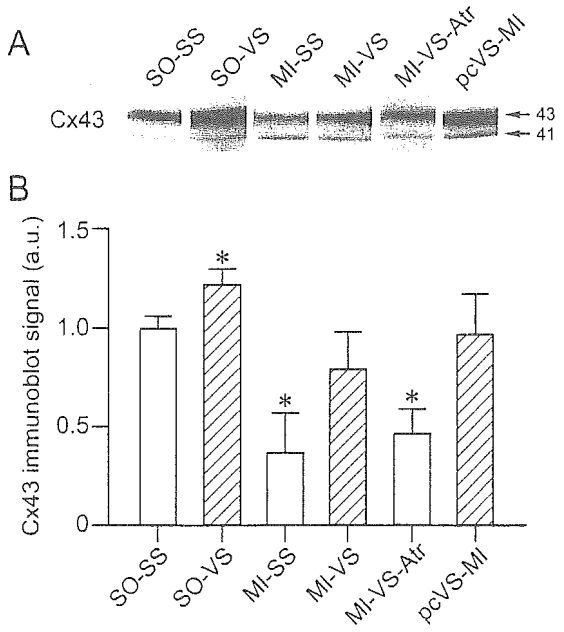

Figure 3. A, Representative immunoblots of homogenate of left ventricles from SO-SS, SO-VS, MI-SS, MI-VS, MI-VS-Atr, and pcVS-MI rats, probed with polyclonal Cx43 antibody. Arrows indicate position of phosphorylated isoform of Cx43 (43 kDa) and nonphosphorylated isoform of Cx43 (41 kDa) bands, respectively. B, Quantitative densitometric analysis of phosphorylated isoform of Cx43 in SO-SS, SO-VS, MI-SS, MI-VS, MI-VS-Atr, and pcMI-VS groups. Data are expressed as mean±SD. a.u. indicates arbitrary units. n=5 for each group. *$P<0.05$.

Effects of Hypoxia and ACh on Intercellular Coupling and Beating Rate

To assess whether the induction of phosphorylated Cx43 by ACh results in a functional effect on cell-to-cell communication, LY dye transfer analysis was performed in primary cultured cardiomyocytes. As shown in Figure 6A, under normoxic conditions, LY injected into a cardiomyocyte diffused into other cardiomyocytes around the injected cell. In contrast, LY injected into a cardiomyocyte under chemical hypoxic conditions was confined to the injected cell, and no dye coupling with other cardiomyocytes was observed (Figure 6B); on the other hand, ACh administration preserved cell-to-cell communication (Figure 6C). Atropine treatment inhibited the preventive effect of ACh on hypoxia-induced uncoupling (Figure 6D). Under normoxic conditions, ACh treatment remarkably induced dye coupling between cardiomyocytes (Figure 6E).

Under normoxic conditions, the rate of spontaneous beating was 62±13 bpm (n=5 experiments), and ACh did not slow the beating rate. Chemical hypoxia with $CoCl_2$ stopped the beating; however, even under hypoxic conditions, ACh preserved spontaneous beating. In the presence of atropine, ACh failed to prevent the hypoxia-induced cessation of beating. The results of Cx43 immunoblotting under chemical hypoxic conditions were identical to those under hypoxia with <2% O_2 (data not shown).

Discussion

In the present study, we investigated whether VS could attenuate acute MI-induced arrhythmogenic properties via modulation of a principal cardiac gap-junction protein, Cx43. Our results provide novel evidence that VS effectively

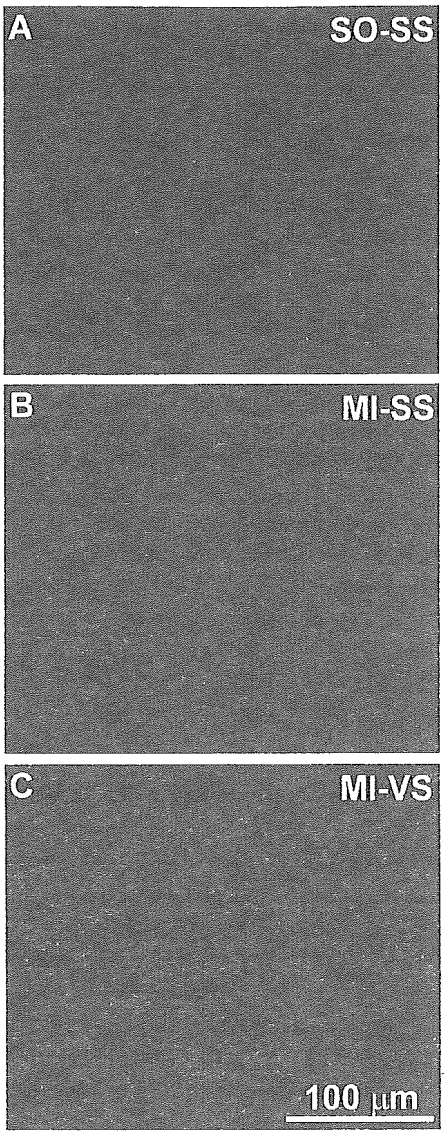

Figure 4. Representative confocal images of rat left ventricles from SO-SS rats (A), MI-SS rats (B), and MI-VS rats (C). Positive immunoreactive signals were concentrated in discrete spots at sites of intercellular apposition (red).

inhibits loss of the phosphorylated isoform of Cx43 during acute MI. Although the precise mechanism by which VS modulates the dephosphorylation of Cx43 remains unknown, it is most likely that VS exerts its antiarrhythmogenic effects on ischemic ventricular myocytes through the preserved function of Cx43.

VS and Antiarrhythmogenic Properties

VS has already been reported to prevent ventricular fibrillation in dogs.[14] In the present study, we hypothesized that VS exerts its antiarrhythmogenic properties by maintaining electrical coupling with ventricular cardiomyocytes as a result of prevention of Cx43 dephosphorylation induced by acute MI. However, because VS simultaneously evokes a bradycardiac effect, the question remains whether the heart rate deceleration caused by VS is a primary mechanism for antiarrhythmic properties during MI. In a preliminary study, we confirmed

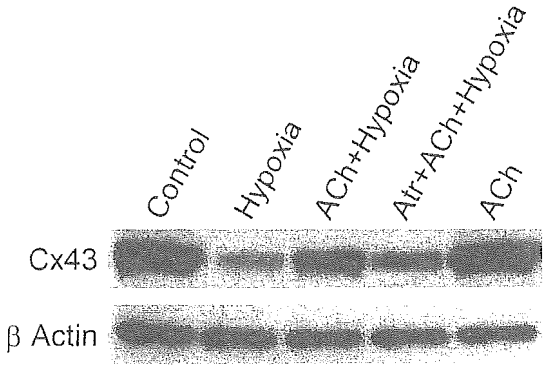

Figure 5. Representative immunoblots of homogenates from primary cultured rat cardiomyocytes probed with polyclonal anti-Cx43 antibody. Hypoxic treatment for 30 minutes decreased phosphorylated Cx43. ACh treatment prevented hypoxia-induced loss of phosphorylated Cx43. Atr inhibited ACh effect. Under normoxic conditions, ACh significantly increased phosphorylated isoform of Cx43 compared with control group.

that short-term exposure of cultured cardiomyocytes to ACh only before hypoxia prevented the hypoxia-induced loss of phosphorylated Cx43 (unpublished observations, 2004). Therefore, it is conceivable that ACh had a cardioprotective effect independent of the heart rate–slowing mechanism during hypoxia or ischemia. To further clarify such a preconditioning effect in in vivo experiments, we examined whether hearts preconditioned by VS were insusceptible to ischemia-induced VT and whether pcVS prevented the ischemia-induced loss of Cx43. As expected, we confirmed that pcVS exerted its antiarrhythmogenic effects and sustained the level of phosphorylated Cx43 during ischemia. These results suggest that VS or ACh had a cardioprotective effect independent of the heart rate–slowing mechanism.

It is well recognized that Cx43, which is the principal component of ventricular gap-junction proteins, contributes to intercellular communication and electrical coupling. Beardslee et al[21] showed that Cx43 underwent marked dephosphorylation during the process of electrical uncoupling induced by ischemia. Genetically engineered Cx43-deficient ($Cx43^{+/-}$ or $Cx43^{-/-}$) mice have been reported to be markedly susceptible to ischemia-induced VT.[12,13,22] In the present study, VS drastically reduced the incidence of VT and prevented the loss of phosphorylated Cx43 during acute MI. Therefore, functional preservation of Cx43 by VS would play an important role in antiarrhythmogenic properties during acute MI.

The result that ACh administration ameliorated the hypoxia-induced loss of dye coupling in cardiomyocytes is consistent with that of ACh-induced upregulation of phosphorylated Cx43. Under normoxic conditions, ACh did not slow down the spontaneous beating rate of cardiomyocytes. Hypoxia stopped the beating and diminished the phosphorylated isoform of Cx43; however, even under hypoxic conditions, ACh preserved the spontaneous beating and the phosphorylated isoform of Cx43. Therefore, it is conceivable that ACh has a cardioprotective effect independent of the beating rate.

Upregulation of Cx43 has been reported to accelerate spontaneous beating in cultured cardiomyocytes.[23] Moreover,

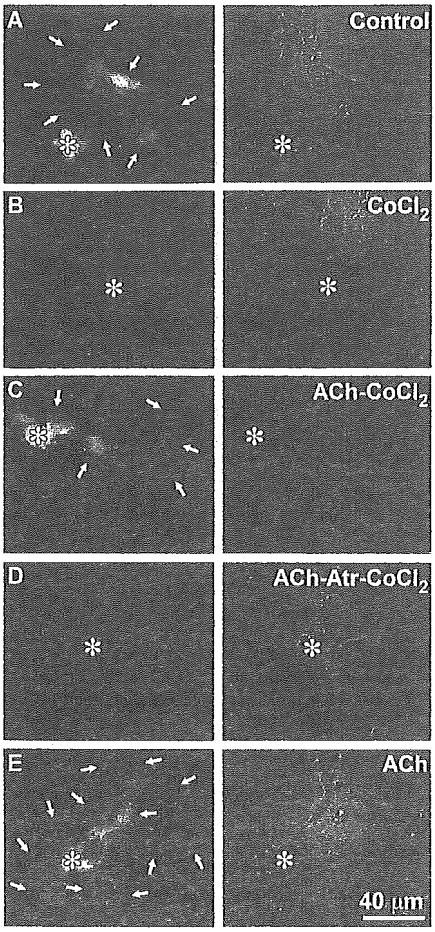

Figure 6. LY dye transfer assay in primary cultured rat cardiomyocytes. Each panel consists of fluorescent micrograph and transmission light micrograph. A, Control cultured cardiomyocytes. B, Cardiomyocytes treated with $CoCl_2$. C, Cardiomyocytes treated with ACh and $CoCl_2$. D, Cardiomyocytes treated with Atr, ACh, and $CoCl_2$. E, Cardiomyocytes treated with ACh alone. Asterisks indicate dye-injected cells; white arrows, coupled neighbors.

cultured cardiomyocytes from genetically engineered Cx43-deficient ($Cx43^{-/-}$) mice demonstrated slow spontaneous beating rates and were poorly synchronized with each other compared with wild-type cultured cardiomyocytes.[24] From these findings and the present results, we speculate that ACh exerts its antiarrhythmogenic properties on ischemic or hypoxic hearts by preserving Cx43 and that such a beneficial effect is independent of its bradycardiac effect.

The spatial distribution of Cx43 can influence electrical stability of the heart. A more recent study by Poelzing and Rosenbaum[11] has shown that the transmural derangement of Cx43 expression can potentially be an arrhythmogenic substrate in the canine model of pacing-induced heart failure. Although we did not evaluate the transmural heterogeneity of Cx43 expression in the present study, such an analysis would be needed to clarify precise mechanisms for the antiarrhythmogenic effects of VS.

How Does VS Modulate Phosphorylated Cx43?

Three potential mechanisms might be involved in the linkage between VS and the sustained phosphorylated-protein level of Cx43 during acute MI. First, VS may activate several protein kinases and induce phosphorylation of Cx43 through muscarinic receptors.[25] Liu et al[26] demonstrated that ACh prevented ischemic injury in cultured cardiomyocytes by activating protein kinase C, and the protective effect was mediated through a nitric oxide–dependent pathway. Second, VS can block the degradation pathway of Cx43 during acute MI. It has been reported that Cx43 is a short-lived protein with a half-life of only 1 to 3 hours in adult hearts[20] and that both lysosomal and proteasomal degradation play distinct roles in the life cycle of Cx43.[27] Our observations in the present study suggest that VS may prevent the ischemia-induced loss of Cx43 as a consequence of inhibition of its degradation pathway. Third, VS is also postulated to suppress excessive inflammation. Recently, Tracey and colleagues[28,29] identified a novel molecular link between the vagus nerve system and an antiinflammatory response to disease. They suggest that VS exerts an antiinflammatory effect via the nicotinic ACh receptor α7-subunit expressed in macrophages. The release of tumor necrosis factor-α from macrophages is inhibited by nicotinic stimulation. In contrast, the present results indicate that VS exerts its antiarrhythmogenic effects via muscarinic cholinergic receptors.

Study Limitations

In the present study, we did not measure the myocardial interstitial level of ACh at the ischemic region during VS. Therefore, it is unclear whether the cardiac vagal efferent fiber innervating the ischemic region can release its neurotransmitter in response to electrical stimulation. An in vivo microdialysis technique has enabled monitoring of the local concentration of neurotransmitters such as catecholamines, amino acids, and ACh. In the cat heart, Kawada et al showed that VS increased the myocardial interstitial ACh level even in the ischemic region (e-mail, February 12, 2004). Although their previous study[30] showed that acute MI induced the nerve-firing independent release of ACh from the vagal terminal, the electrical stimulation of the vagal efferent during acute MI produced the significant additive release of ACh to the myocardial interstitial space. Such an additional release of ACh in response to electrical stimulation during acute MI would play an important role in Cx43 preservation in the ischemic region.

Conclusion and Future Aspects

The present study demonstrates that VS exerts antiarrhythmogenic effects during acute MI accompanied by prevention of the loss of phosphorylated Cx43. The preserved function of Cx43 may improve electrical instability during acute MI. In view of the present results, we can provide an alternative therapeutic strategy with a neural interface approach. We have already developed the sympathetic interface approach for the treatment of central baroreflex failure in rats.[31] To establish the therapeutic strategy shown here, further studies are required.

Acknowledgments

This study was supported by Health and Labor Sciences Research Grant (H15-PHYSI-001) for Advanced Medical Technology from

the Ministry of Health, Labor and Welfare of Japan. We thank Ken-ichi Yagyu for his technical assistance.

References

1. Zipes DP, Wellens HJ. Sudden cardiac death. *Circulation.* 1998;98: 2334–2351.
2. Mehta D, Curwin J, Gomes JA, Fuster V. Sudden death in coronary artery disease: acute ischemia versus myocardial substrate. *Circulation.* 1997; 96:3215–3223.
3. Smith WT IV, Fleet WF, Johnson TA, Engle CL, Cascio WE. The Ib phase of ventricular arrhythmias in ischemic in situ porcine heart is related to changes in cell-to-cell electrical coupling. *Circulation.* 1995; 92:3051–3060.
4. Cinca J, Blanch P, Carreno A, Mont L, Garcia-Burillo A, Soler-Soler J. Acute ischemic ventricular arrhythmias in pigs with healed myocardial infarction: comparative effects of ischemia at a distance and ischemia at the infarct zone. *Circulation.* 1997;96:653–658.
5. Saffitz JE, Schuessler RB, Yamada KA. Mechanisms of remodeling of gap junction distributions and the development of anatomic substrates of arrhythmias. *Cardiovasc Res.* 1999;42:309–317.
6. Severs NJ. Gap junction remodeling in heart failure. *J Card Fail.* 2002; 8:S293–S299.
7. Dhein S, Polontchouk L, Salameh A, Haefliger JA. Pharmacological modulation and differential regulation of the cardiac gap junction proteins connexin 43 and connexin 40. *Biol Cell.* 2002;94:409–422.
8. Peters NS, Green CR, Poole-Wilson PA, Severs NJ. Reduced content of connexin43 gap junctions in ventricular myocardium from hypertrophied and ischemic human hearts. *Circulation.* 1993;88:864–875.
9. Kaprielian RR, Gunning M, Dupont E, Sheppard MN, Rothery SM, Underwood R, Pennell DJ, Fox K, Pepper J, Poole-Wilson PA, Severs NJ. Downregulation of immunodetectable connexin43 and decreased gap junction size in the pathogenesis of chronic hibernation in the human left ventricle. *Circulation.* 1998;97:651–660.
10. Spragg DD, Leclercq C, Loghmani M, Faris OP, Tunin RS, DiSilvestre D, McVeigh ER, Tomaselli GF, Kass DA. Regional alterations in protein expression in the dyssynchronous failing heart. *Circulation.* 2003;108: 929–932.
11. Poelzing S, Rosenbaum DS. Altered connexin43 expression produces arrhythmia substrate in heart failure. *Am J Physiol.* 2004;287: H1762–H1770.
12. Lerner DL, Yamada KA, Schuessler RB, Saffitz JE. Accelerated onset and increased incidence of ventricular arrhythmias induced by ischemia in Cx43-deficient mice. *Circulation.* 2000;101:547–552.
13. Gutstein DE, Morley GE, Tamaddon H, Vaidya D, Schneider MD, Chen J, Chien KR, Stuhlmann H, Fishman GI. Conduction slowing and sudden arrhythmic death in mice with cardiac-restricted inactivation of connexin43. *Circ Res.* 2001;88:333–339.
14. Vanoli E, De Ferrari GM, Stramba-Badiale M, Hull SS Jr, Foreman RD, Schwartz PJ. Vagal stimulation and prevention of sudden death in conscious dogs with a healed myocardial infarction. *Circ Res.* 1991;68: 1471–1481.
15. Li M, Zheng C, Sato T, Kawada T, Sugimachi M, Sunagawa K. Vagal nerve stimulation markedly improves long-term survival after chronic heart failure in rats. *Circulation.* 2004;109:120–124.
16. Engelstein ED. Prevention and management of chronic heart failure with electrical therapy. *Am J Cardiol.* 2003;91:62F–73F.
17. DiBona GF, Sawin LL. Reflex regulation of renal nerve activity in cardiac failure. *Am J Physiol.* 1994;266:R27–R39.
18. Kikuchi H, Fujinawa T, Kuribayashi F, Nakanishi A, Imajoh-Ohmi S, Goto M, Kanegasaki S. Induction of essential components of the superoxide generating system in human monoblastic leukemia U937 cells. *J Biochem.* 1994;116:742–746.
19. Chun YS, Hyun JY, Kwak YG, Kim IS, Kim CH, Choi E, Kim MS, Park JW. Hypoxic activation of the atrial natriuretic peptide gene promoter through direct and indirect actions of hypoxia-inducible factor-1. *Biochem J.* 2003;370:149–157.
20. Beardslee MA, Laing JG, Beyer EC, Saffitz JE. Rapid turnover of connexin43 in the adult rat heart. *Circ Res.* 1998;83:629–635.
21. Beardslee MA, Lerner DL, Tadros PN, Laing JG, Beyer EC, Yamada KA, Kleber AG, Schuessler RB, Saffitz JE. Dephosphorylation and intracellular redistribution of ventricular connexin43 during electrical uncoupling induced by ischemia. *Circ Res.* 2000;87:656–662.
22. Yao JA, Gutstein DE, Liu F, Fishman GI, Wit AL. Cell coupling between ventricular myocyte pairs from connexin43-deficient murine hearts. *Circ Res.* 2003;93:736–743.
23. Ai Z, Fischer A, Spray DC, Brown AM, Fishman GI. Wnt-1 regulation of connexin43 in cardiac myocytes. *J Clin Invest.* 2000;105:161–171.
24. Vink MJ, Suadicani SO, Vieira DM, Urban-Maldonado M, Gao Y, Fishman GI, Spray DC. Alterations of intercellular communication in neonatal cardiac myocytes from connexin43 null mice. *Cardiovasc Res.* 2004;62:397–406.
25. van Koppen CJ, Kaiser B. Regulation of muscarinic acetylcholine receptor signaling. *Pharmacol Ther.* 2003;98:197–220.
26. Liu H, McPherson BC, Zhu X, Da Costa ML, Jeevanandam V, Yao Z. Role of nitric oxide and protein kinase C in ACh-induced cardioprotection. *Am J Physiol.* 2001;281:H191–H197.
27. Qin H, Shao Q, Igdoura SA, Alaoui-Jamali MA, Laird DW. Lysosomal and proteasomal degradation play distinct roles in the life cycle of Cx43 in gap junctional intercellular communication-deficient and -competent breast tumor cells. *J Biol Chem.* 2003;278:30005–30014.
28. Tracey KJ. The inflammatory reflex. *Nature.* 2002;420:853–859.
29. Wang H, Yu M, Ochani M, Amella CA, Tanovic M, Susarla S, Li JH, Wang H, Yang H, Ulloa L, Al-Abed Y, Czura CJ, Tracey KJ. Nicotinic acetylcholine receptor alpha7 subunit is an essential regulator of inflammation. *Nature.* 2003;421:384–388.
30. Kawada T, Yamazaki T, Akiyama T, Sato T, Shishido T, Inagaki M, Takaki H, Sugimachi M, Sunagawa K. Differential acetylcholine release mechanisms in the ischemic and non-ischemic myocardium. *J Mol Cell Cardiol.* 2000;32:405–414.
31. Sato T, Kawada T, Sugimachi M, Sunagawa K. Bionic technology revitalizes native baroreflex function in rats with baroreflex failure. *Circulation.* 2002;106:730–734.

CLINICAL PERSPECTIVE

Increased cardiac vagal tone reduces ventricular arrhythmias during acute myocardial ischemia and has been linked to a lower risk of sudden arrhythmic death. Although the benefit of bradycardia associated with vagal tone is well appreciated, this may not be the only benefit. Cardiomyocytes are electrically coupled to one another through gap junctions. This coupling is critical to maintenance of cardiac electrical stability. Uncoupling occurs during ischemia and promotes heterogeneity of repolarization and slowing of conduction, with proarrhythmic effects. In the present study, short-term vagal stimulation (VS) was applied before or during acute ischemia in rats. VS protected against ventricular arrhythmias. Furthermore, VS preserved a phosphorylated form of connexin 43 (Cx43), a major subtype of gap-junction proteins in ventricles. In vitro studies of rat primary-cultured cardiomyocytes showed that ACh, a vagal efferent neurotransmitter, effectively prevented hypoxia-induced loss of phosphorylated Cx43 proteins and maintained cell-to-cell communication. Antiarrhythmic properties of VS and ACh were mediated via muscarinic receptors but were independent of heart rate deceleration. That cellular coupling can be improved through neural stimulation may lead to novel therapeutic strategies for preventing ventricular fibrillation during ischemia.

Journal of Human Hypertension (2005) 19, 527–533

www.nature.com/jhh

ORIGINAL ARTICLE

Association between arterial stiffness and platelet activation

F Yamasaki[1], T Furuno[2], K Sato[2], D Zhang[3], M Nishinaga[2], T Sato[3], Y Doi[2] and T Sugiura[1]
[1]*Department of Clinical Laboratory, Kochi Medical School, Nankoku, Kochi, Japan;* [2]*Department of Medicine and Geriatrics, Kochi Medical School, Nankoku, Kochi, Japan;* [3]*Department of Cardiovascular Control, Kochi Medical School, Nankoku, Kochi, Japan*

Increased arterial stiffness is strongly associated with atherosclerosis, while platelet activation is an important trigger of thrombotic events in patients with atherosclerosis. However, little is known about the effect of arterial stiffness on platelet activation. We therefore investigated the association between arterial stiffness and platelet activation in 38 normal volunteers (20 men and 18 women) aged 23–77 years (mean = 49 ± 15 years). Arterial stiffness was assessed by measuring brachial–ankle pulse wave velocity (ba-PWV) and heart–brachial PWV (hb-PWV). Flow cytometric analyses were performed to evaluate platelet activation by measuring surface expression of P-selectin and platelet–neutrophil complexes (PNC) before and after activation by ADP. We also calculated the difference between basal and stimulated states of P-selectin and PNC to assess platelet activation reserve. PWVs were significantly correlated with age and BP ($r = 0.60$–0.81). For platelet activation and activation reserve, correlations with age were less strong but remained significant ($r = 0.36$–0.61), with the exception of P-selectin (not significant, NS), and correlations with SBP were similar ($r = 0.35$–0.53). A significant correlation was found between PWVs and platelet activation ($r = 0.43$–0.74). Multiple regression analysis demonstrated significant correlations between platelet activation and reserve and PWVs (coefficient = 2.17–6.59), when both age and BP were adjusted for simultaneously. In conclusion, platelet activation was associated with arterial stiffness, suggesting that arterial stiffness may play an important role in thrombotic events.
Journal of Human Hypertension (2005) 19, 527–533.
doi:10.1038/sj.jhh.1001861
Published online 7 April 2005

Keywords: arterial stiffness; pulse wave velocity; P-selectin; platelet–neutrophil complexes

Introduction

Platelet activation and aggregation are important triggers of thrombotic events in patients with atherosclerosis. In such patients, platelets are activated at the site of atheroma[1] due to increased shear stress in the narrowed vessels.[2,3] Increased platelet activation is observed in patients with coronary risk factors and cardiovascular events.[4–12]

Increased arterial stiffness, measured with pulse wave velocity (PWV), has been shown to be associated with atherosclerosis and risk factors of atherosclerotic cardiovascular disease,[13–21] and is an independent predictor of cardiovascular events.[22,23] Therefore, although platelets are likely to be activated in patients with atherosclerotic disease who exhibit increased arterial stiffness, little is known about the relation of arterial stiffness itself to platelet activation.

Recently, platelet activation has been widely evaluated by measuring soluble P-selectin; a platelet surface molecule also termed CD62P.[4,6–8,11] Although the measurement of soluble P-selectin is simple and useful, it is an indirect method of evaluating platelet activation. On the other hand, platelet activation can be detected directly by measuring surface antigen CD62P using flow cytometry.[2,3,5,9,10,12] Furthermore, detection of platelet–neutrophil complexes (PNC), which are formed as a result of interaction with CD62P provides an additional means to detect platelet activation.[24]

The purpose of this study was to investigate the association between arterial stiffness and platelet activation by measuring PWV, P-selectin, and PNC in subjects without atherosclerotic disease.

Materials and methods

Subjects

We studied 38 healthy nonsmoking volunteers (20 men and 18 women), aged 23–77 years

Correspondence: Dr F Yamasaki, Department of Clinical Laboratory, Kochi Medical School, Nankoku, Kochi 783-8505, Japan.
E-mail: yamasakf@kochi-ms.ac.jp
This research was supported in part by a grant from the President Research Fund of Kochi Medical School Hospital and the Japan Arteriosclerosis Prevention Fund.
Received 15 March 2004; revised 5 January 2005; accepted 9 February 2005; published online 7 April 2005

(mean = 49 ± 15 years) with no evidence of heart disease on physical examination, standard 12-lead electrocardiography, chest radiography, echocardiography, or blood chemistry analysis. Subjects had no self-reported past history or current evidence of cardiovascular disease, hypertension, hypercholesterolaemia, diabetes mellitus or renal disease. Basic characteristics of subjects are shown in Table 1. None of the subjects had frequent ectopic beats or atrial fibrillation and none had taken any medication for at least 10 days. Informed consent was obtained before performing the study and the study protocol was approved by the Local Ethics Committee of Kochi Medical School.

Evaluation of arterial stiffness

Arterial stiffness was evaluated by PWV, measured using volume-plethysmographic apparatus (Colin, Komaki, Japan).[18–21] Data were acquired with subjects lying supine in a quiet and temperature-controlled room at 11 AM, at least 3 h after breakfast. Surface electrodes were attached to both wrists for ECG measurement, a microphone was positioned at the left sternal edge to detect heart sounds, and cuffs incorporating plethysmographic and oscillometric sensors were fastened around both the brachial regions and ankles to measure pulse wave forms and blood pressure. Brachial–ankle PWV (ba-PWV) and heart–brachial PWV (hb-PWV) were measured as follows. The time interval between the wave foot of the brachial waveform and that of the ankle waveform was defined as the time interval between the brachial region and ankle, while the time interval between the heart and the right brachial artery was defined as the time interval between the second heart sound and the right brachial waveform. The distance between these sampling points was calculated automatically according to the height of the subject. PWVs were calculated by dividing each distance by the respective time interval. Right brachial blood pressure (systolic and diastolic) and pulse rate were concurrently measured.

Table 1 Clinical characteristics of subjects

Parameters	*All subjects (n = 38)*
Age (years)	49 ± 15
Gender, male/female	20/18
Systolic blood pressure (mmHg)	125 ± 16
Diastolic blood pressure (mmHg)	77 ± 10
Pulse rate (bpm)	66 ± 10
Blood sugar (mg/dl)	98.5 ± 18.5
Total cholesterol (mg/dl)	192.6 ± 20.7
Blood urea nitrogen (mg/dl)	14.0 ± 18.5
Creatinine (mg/dl)	0.69 ± 0.15
PNC (%)	9.5 ± 4.9
PNC(ADP) (%)	20.2 ± 9.9
Δ-PNC	10.7 ± 6.9
P-selectin (%)	13.1 ± 1.7
P-selectin(ADP) (%)	36.6 ± 9.2
Δ-P-selectin	23.6 ± 9.1
hb-PWV (m/s)	5.3 ± 0.9
ba-PWV (m/s)	13.8 ± 3.0

Values are expressed as mean ± s.d.
PNC = platelet neutrophil complexes; ADP = adenosine diphosphate; Δ-PNC = PNC (ADP)−PNC; Δ-P-selectin = P-selectin (ADP)−P-selectin; hb-PWV = heart–brachial pulse wave velocity; ba-PWV = brachial–ankle pulse wave velocity.

Measurement of platelet activation

Sample preparation and measurement of platelet P-selectin (CD62P) and PNC levels were performed according to the method described by Peters *et al*.[24] To minimize platelet activation during blood collection, blood was drawn via a 21 G butterfly needle without the use of a tourniquet. After discarding the first 2 ml of blood, a further 2 ml was collected and immediately added to 200 μl of sodium citrate (3.13%). All antibodies were sourced as follows: Fluorescein isothiocyanate (FITC) labelled IgG1 anti-CD62P from Dainippon Pharmaceutical, Osaka, Japan, phycoerythin (PE) labelled IgG2a anti-CD42b and FITC labelled IgG1 anti-CD11b from Beckman Coulter, Fullerton, CA, USA. As negative controls, FITC-labelled IgG1 (Beckman Coulter, Fullerton, CA, USA) and double-stained (FITC/PE) IgG1 and IgG2a (Dako, High Wycombe, Bucks, UK) irrelevant antibodies were included.

Sample preparation for the measurement of platelet CD62P level: In all, 5 μl of blood was added to a round-bottomed polystyrene tube containing 50 μl of platelet buffer (10 mmol/l HEPES, 145 mmol/l NaCl, 5 mmol/l KCl, 1 mmol/l $MgSO_4$; pH 7.4), and 5 μl of anti-CD62P or control IgG1 antibody. Following gentle suspension, samples were incubated in the dark at room temperature for 20 min without stirring. Then 250 μl of fixative was added and the tubes were incubated for an additional 10 min. The samples were then diluted with 500 μl of buffer and analysed. Flow cytometric analysis was performed within 1 h of fixation.

Sample preparation for the measurement of PNC level: In all, 50 μl of blood was added to a round-bottomed polystyrene tube containing 5 μl of anti-CD42b, and 5 μl of anti-CD11b or isotype control antibodies. Following gentle mixing, samples were incubated in the dark at room temperature for 10 min without stirring. Then 500 μl of fixative was added and the tubes were incubated for additional 10 min. Flow cytometric analysis was performed within 1 h of preparation.

Flow cytometric analysis

Blood samples were analysed in a COULTER EPICS XL Profile Flow Cytometer, Miami, FL, USA, using either single or double fluorochromes. The peak emission intensity of FITC fluorescence was

detected at 515 nm and that of phycoerythin fluorescence at 580 nm.

Measurement of platelet CD62P level: After forward and side scatter measurements were made with gain setting in logarithmic mode, platelet-sized events were counted. CD62P-positive platelets were defined as those with a fluorescence intensity exceeding that of 98% of the platelets staining with control antibody.

Measurement of PNC level: After forward and side scatter measurements were made with gain setting in linear mode, neutrophil-sized events were selected. Results were defined as positive when the fluorescence intensity exceeded that of 98% of the isotype-matched (IgG1 and IgG2a) control antibodies staining. Events positive for both CD11b and CD42b were considered to represent PNCs and were expressed as percentages of events with positive CD11b staining.

Evaluation of platelet activation reserve: We evaluated platelet activation reserve, that is, the ability of the platelets to be activated, in a separate experiment. Platelets were activated with 5 μl of adenosine diphosphate (ADP). We also calculated the difference between basal and stimulated states of P-selectin expression (Δ-P-selectin) and PNC level (Δ-PNC) to determine activation reserve.

Statistical analysis

Data are presented as mean ± s.d. Univariate linear correlation analysis and multiple regression analysis were used for statistical evaluation. The variables significantly associated with platelet activation on univariate analysis were included in a multiple regression analysis in order to adjust PWV for each variable. Gender differences were evaluated with ANOVA. *P*-values <0.05 were considered to represent statistical significance.

Results

Both ba-PWV and hb-PWV exhibited significant positive correlations with age, systolic, and diastolic blood pressure ($r=0.60$–0.81, $P<0.05$ or <0.01), and pulse rate ($r=0.44$, $P<0.05$, $r=0.65$, <0.01, respectively) (Table 2). For platelet activation and activation reserve, correlations with age were less strong but remained significant ($r=0.36$–0.61, $P<0.05$ or <0.01) with the exception of Δ-P-selectin (not significant, NS), and correlations with systolic and diastolic blood pressure were similar ($r=0.35$–0.53, $P<0.05$ or <0.01) with the exception of P-selectin (NS) (Table 3). However, platelet activation and activation reserve exhibited no significant correlation with pulse rate, blood glucose, total cholesterol, blood urea nitrogen or creatinine. No significant gender-related differences were observed in any of these correlations (Tables 2 and 3).

Table 2 Correlation between PWV and clinical indices

	hb-PWV	*ba-PWV*
Age	0.74**	0.80**
Systolic blood pressure	0.61**	0.81**
Diastolic blood pressure	0.60**	0.74**
Pulse rate	0.44*	0.65**
Blood sugar	−0.05	−0.17
Total cholesterol	−0.03	−0.30
Blood urea nitrogen	−0.32	0.32
Creatinine	0.04	−0.14
Gender		
Male	5.5 ± 1.0	14.1 ± 3.0
Female	5.2 ± 0.8	13.6 ± 3.1

PNC = platelet neutrophil complexes; ADP = adenosine diphosphate; Δ-PNC = PNC (ADP) − PNC; Δ-P-selectin = P-selectin (ADP) − P-selectin; hb-PWV = heart–brachial pulse wave velocity; ba-PWV = brachial–ankle pulse wave velocity.
For parameters from age to creatinine, values are correlation coefficients.
*$P<0.05$.
**$P<0.01$.
For gender, values are mean ± s.d., with differences evaluated with ANOVA.

PWVs exhibited significant positive correlations ($r=0.43$–0.74, $P<0.05$ or <0.01) to all indices of platelet activation and reserve (Table 4, Figure 1). When age or blood pressures were adjusted for on multivariate analysis, some indices of platelet activation and reserve were significantly related to PWVs ($r=0.34$–7.67, $P<0.05$ or <0.01). When both age and blood pressures were simultaneously adjusted for, significant correlations remained between platelet activation and reserve and PWVs ($r=2.17$–6.59, $P<0.05$ or <0.01) (Table 4). In other words, although the relationship between PWVs and the indices of platelet activation was strongly affected by age and blood pressure, a significant association remained when these factors were adjusted for.

Discussion

The main finding of this study was that platelet activation and activation reserve were associated with arterial stiffness when analyses were adjusted for age and blood pressure. This suggests that increased arterial stiffness might play an important role in thrombotic events.

Patients with hypertension, cerebrovascular disease, coronary heart disease, diabetes mellitus, and renal failure are recognized to have less arterial compliance than normal subjects.[13–15,17–19] Increased PWV has also been reported to be an independent predictor of cardiovascular events in patients with hypertension or renal failure, and in elderly subjects.[22,23] The association between increased arterial stiffness and high incidence of cardiovascular events may be explained by the existence of atherosclerosis. Hirai *et al*[25] have demonstrated strong associations between abdominal aortic and

Table 3 Correlation between platelet activation and clinical indices

	PNC	*PNC (ADP)*	*Δ-PNC*	*P-selectin*	*P-selectin (ADP)*	*Δ-P-selectin*
Age	0.51**	0.61**	0.52**	0.36*	0.38*	0.32
Systolic blood pressure	0.41*	0.53**	0.48**	0.41*	0.43*	0.35*
Diastolic blood pressure	0.43*	0.49**	0.40*	0.25	0.40*	0.36*
Pulse rate	0.28	0.25	0.16	0.04	0.15	0.15
Blood sugar	0.09	−0.18	−0.31	−0.17	0.13	0.16
Total cholesterol	−0.14	−0.07	0.001	−0.10	−0.13	−0.11
Blood urea nitrogen	−0.01	0.12	0.18	−0.05	0.05	0.06
Creatinine	0.05	−0.13	−0.22	0.04	−0.17	−0.18
Gender						
Male	10.3±5.9	19.7±8.7	9.4±6.9	13.1±1.8	35.5±9.3	22.4±9.0
Female	8.8±3.8	20.7±11.4	11.9±6.8	13.0±1.7	37.7±9.2	24.7±9.3

PNC = platelet neutrophil complexes; ADP = adenosine diphosphate; Δ-PNC = PNC (ADP)−PNC; Δ-P-selectin = P-selectin (ADP)−P-selectin; hb-PWV = heart–brachial pulse wave velocity; ba-PWV = brachial–ankle pulse wave velocity.
For parameters from age to creatinine, values are correlation coefficients.
*$P<0.05$.
**$P<0.01$.
For gender, values are mean±s.d., with differences evaluated with ANOVA.

Table 4 Relation between platelet activations and PWV

	PNC	*PNC (ADP)*	*Δ-PNC*	*P-selectin*	*P-selectin (ADP)*	*Δ-P-selectin*
Not adjusted						
hb-PWV	0.62**	0.74**	0.63**	0.45**	0.57**	0.50**
ba-PWV	0.59**	0.71**	0.61**	0.47**	0.51**	0.43*
Adjusted for age						
hb-PWV	2.86**	6.95**	4.09*	0.75	6.55**	5.80*
ba-PWV	0.79	2.01**	1.22*	0.28	1.75*	1.47
Adjusted for systolic blood pressure						
hb-PWV	3.20**	7.23**	4.04**	0.59	5.09*	4.50*
ba-PWV	1.21**	2.64**	1.44*	0.23	1.48	1.25
Adjusted for diastolic blood pressure						
hb-PWV	3.08**	7.67**	4.59**	0.87*	5.32**	4.46*
ba-PWV	0.97**	2.50**	1.54**	0.34*	1.45*	1.10
Adjusted for age and systolic blood pressure						
hb-PWV	2.80*	6.43**	3.63*	0.58	5.93*	5.35*
ba-PWV	1.08	2.32*	1.24	0.24	1.72	1.48
Adjusted for age and diastolic blood pressure						
hb-PWV	2.63*	6.59**	3.97**	0.78	6.06*	5.28*
ba-PWV	0.76	2.17*	1.40	0.40	1.66	1.26

PNC = platelet neutrophil complexes; ADP = adenosine diphosphate; Δ-PNC = PNC (ADP)−PNC; Δ-P-selectin = P-selectin (ADP)−P-selectin; hb-PWV = heart–brachial pulse wave velocity; ba-PWV = brachial–ankle pulse wave velocity.
'Not adjusted' — values are correlation coefficients between PWVs and indices of platelet activation before adjustment.
*$P<0.05$.
**$P<0.01$.
Other values are regression coefficients between PWVs and indices of platelet activation adjusted for age and/or blood pressures as indicated.
*$P<0.05$.
**$P<0.01$.

carotid arterial stiffness and the degree of coronary artery disease. Popele *et al*[26] recently reported that aortic stiffness as measured by PWV is strongly associated with common carotid intima-media thickness, carotid arterial plaques, and the presence of peripheral arterial disease. Moreover, some population-based studies have demonstrated higher blood pressure, increased age, and male gender to be associated with increased PWV.[16,20,21] Pulse pressure may also relate to arterial stiffness and cardiovascular events, with higher pulse pressure reflecting elevated systolic pressure and reduced diastolic pressure due to increased arterial stiffness. In the present study, significant relationships were observed between PWVs and age, blood pressure, and pulse rate, in accordance with previous studies.

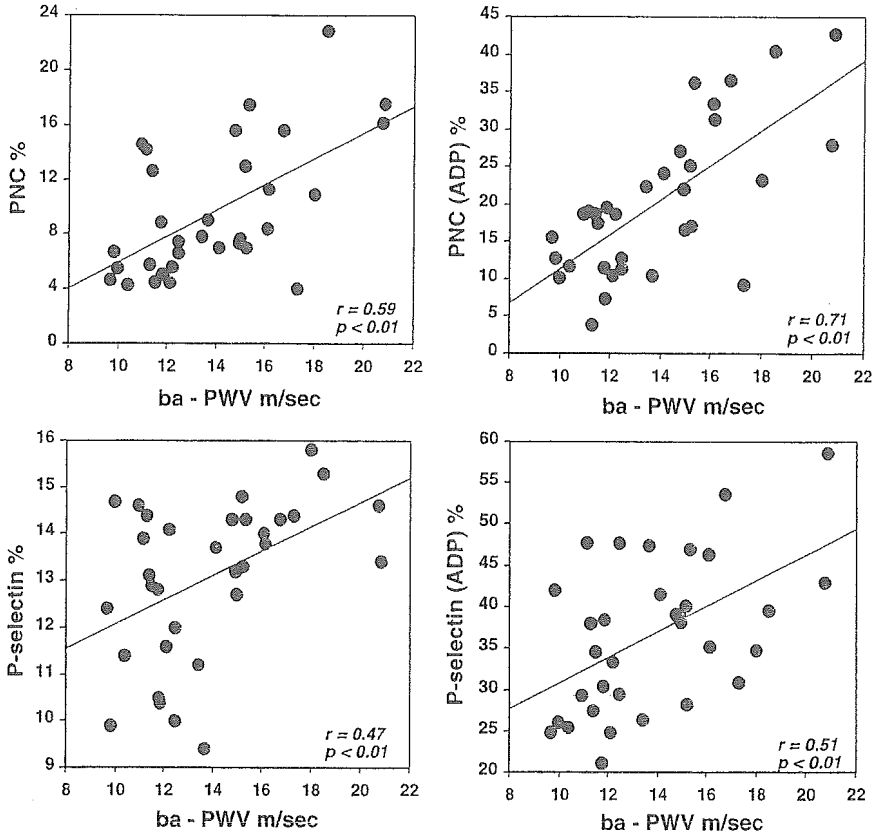

Figure 1 Correlation between ba-PWV and PNC (upper two panels). PNC = platelet neutrophil complexes; ADP = adenosine diphosphate; Δ-PNC = PNC (ADP)−PNC; Δ-P-selectin = P-selectin (ADP)−P-selectin; hb-PWV = heart–brachial pulse wave velocity; ba-PWV = brachial–ankle pulse wave velocity.

P-selectin is a component of α-granules that is expressed on the platelet surface membrane and released into the plasma upon platelet activation. Although the bulk of circulating soluble P-selectin appears to be platelet derived,[27] the substance is also found in the Weibel–Palade bodies of endothelial cells.[28] Direct measurement of platelet membrane P-selectin is therefore a more sensitive method of assessing platelet activation. In the present study, we evaluated platelet activation by measuring membrane activation markers using flow cytometry with activation-dependent monoclonal antibodies. PNC levels were also measured using the same method. P-selectin levels in our normal subjects aged 49±15 years were 13.1±1.7%; this was higher than that in quoted by other studies, possibly due to the differences in monoclonal antibodies or in sample manipulation.

P-selectin expressed on activated platelets causes formation of PNC. Moreover, platelets and platelet-derived P-selectin play an important role in thrombus growth at the site of atherosclerosis.[2] *In vivo* and *in vitro* studies have shown that shear stress and exposure to atherogenic stimuli, such as oxidization by low-density lipoprotein or cigarette smoking, induce rapid P-selectin-dependent aggregation and accumulation of leukocytes and platelets.[4,5,11] Activated platelets accumulating in thrombi at the site of ruptured atherosclerotic plaques will express CD62P. In clinical studies, P-selectin has been shown to be a marker of platelet activation related to adverse cardiovascular events such as hypertension, coronary artery disease, cerebrovascular disease, and peripheral arterial disease,[6,7,10–12] and also to be a predictor of cardiovascular events.[8,12] PNC, forming as a result of the interaction of platelet P-selectin and neutrophils also promotes platelet activation.[24] This is the first study to demonstrate that P-selectin and PNC were significantly correlated with arterial stiffness evaluated by PWV in normal subjects. In an analysis of four randomized trials, Hebert *et al*[29] showed that aspirin therapy was beneficial in the primary prevention of vascular disease. Higher levels of other membrane markers such as von Willebrand factor receptor are observed in activated platelets, which are affected by aspirin or ticlopidine.[30] Therefore, our results indicate that, in the normal population, antiplatelet agents may play a role in preventing cardiovascular events through factors other than P-selectin.

Although the exact mechanism accounting for the relationship between platelet activation and arterial stiffness is unknown, it is possible to make

the following speculations. When arterial stiffness is raised, shear stress might play an important role in platelet activation. Using cone-plate viscometry,[3] Goto *et al* showed that platelet activation (measured by P-selectin surface expression, von Willebrand factor-mediated platelet aggregation and translocation of GP Ibα) was induced by high shear rate of $10\,800\,s^{-1}$. Higher arterial stiffness increases blood flow velocity and produces a steep systolic pressure waveform,[31] and it is possible that the resulting increased shear stress could promote platelet activation. Another possible mechanism is that endothelial dysfunction may interact with arterial stiffness and platelet hyperactivity. Kobayashi *et al*[32] showed significant correlation between endothelial dysfunction measured by flow-mediated dilatation and ba-PWV. Platelets are also activated by endothelial dysfunction. On the other hand, activated platelets themselves may cause arterial stiffness via vascular smooth muscle cell growth factors and extracellular matrix modulator released from platelets, that is, PDGF.[33] However, this response also occurs at the site of endothelial injury. Further study is therefore required to clarify whether arterial stiffness causes platelet activation or alternatively whether platelet activation might result in arterial stiffness.

Limitations

Despite the small sample size, it is possible that the broad age range (23–77 years) of our subjects caused outliers in PWV and platelet activation. However, significant correlations were found when age and blood pressure were adjusted for, suggesting that the influence of age did not entirely explain the correlation between PWV and platelet activation. In the present study, ba-PWV was 14.1 ± 3.0 m/s in men and 13.6 ± 3.1 m/s in women; values higher than those reported by Yamashina *et al*.[20] Furthermore, it is not known whether such a relationship between arterial stiffness and platelet activation is found in patients with conditions such as hypertension, diabetes mellitus, coronary heart disease, and stroke. Further studies should be therefore performed in such patients, using larger sample sizes.

Acknowledgements

We would like to thank Tadashi Ueta for technical assistance and Misa Nakagawa for her assistance throughout the study.

References

1 Tenaglia AN *et al*. Levels of expression of P-selectin, E-selectin, and intercellular adhesion molecule-1 in coronary atherectomy specimens from patients with stable and unstable angina pectoris. *Am J Cardiol* 1997; **79**: 742–747.
2 Hagberg IA, Roald HE, Lyberg T. Platelet activation in flowing blood passing growing arterial thrombi. *Arterioscler Thromb Vasc Biol* 1997; **17**: 1331–1336.
3 Goto S *et al*. Effects of ticlopidine on von Willebrand factor-mediated shear-induced platelet activation and aggregation. *Platelets* 2001; **12**: 406–414.
4 Davi G *et al*. Increased levels of soluble P-selectin in hypercholesterolemic patients. *Circulation* 1998; **97**: 953–957.
5 Pernerstorfer T *et al*. Low-dose aspirin does not lower *in vivo* platelet activation in healthy smokers. *Br J Haematol* 1998; **102**: 1229–1231.
6 Spencer CG *et al*. Von Willebrand factor, soluble P-selectin, and target organ damage in hypertension: a substudy of the Anglo-Scandinavian Cardiac Outcomes Trial (ASCOT). *Hypertension* 2002; **40**: 61–66.
7 Blann AD, Dobrotova M, Kubisz P, McCollum CN. von Willebrand factor, soluble P-selectin, tissue plasminogen activator and plasminogen activator inhibitor in atherosclerosis. *Thromb Haemost* 1995; **74**: 626–630.
8 Blann AD, Faragher EB, McCollum CN. Increased soluble P-selectin following myocardial infarction: a new marker for the progression of atherosclerosis. *Blood Coagul Fibrinolysis* 1997; **8**: 383–390.
9 Grau AJ *et al*. Increased fraction of circulating activated platelets in acute and previous cerebrovascular ischemia. *Thromb Haemost* 1998; **80**: 298–301.
10 Serebruany VL *et al*. Uniform platelet activation exists before coronary stent implantation despite aspirin therapy. *Am Heart J* 2001; **142**: 611–616.
11 Parker III C, Vita JA, Freedman JE. Soluble adhesion molecules and unstable coronary artery disease. *Atherosclerosis* 2001; **156**: 417–424.
12 Lip GY *et al*. Sequential alterations in haemorheology, endothelial dysfunction, platelet activation and thrombogenesis in relation to prognosis following acute stroke: The West Birmingham Stroke Project. *Blood Coagul Fibrinolysis* 2002; **13**: 339–347.
13 De Cesaris R, Ranieri G, Filitti V, Andriani A. Large artery compliance in essential hypertension. Effects of calcium antagonism and beta-blocking. *Am J Hypertens* 1992; **5**: 624–628.
14 Asmar R *et al*. Assessment of arterial distensibility by automatic pulse wave velocity measurement. Validation and clinical application studies. *Hypertension* 1995; **26**: 485–490.
15 Lehmann ED, Riley WA, Clarkson P, Gosling RG. Non-invasive assessment of cardiovascular disease in diabetes mellitus. *Lancet* 1997; **350**Suppl 1: SI14–SI19.
16 Asmar J *et al*. Arterial stiffness and cardiovascular risk factors in a population-based study. *J Hypertens* 2001; **19**: 381–387.
17 Mourad JJ *et al*. Creatinine clearance, pulse wave velocity, carotid compliance and essential hypertension. *Kidney Int* 2001; **59**: 1334–1341.
18 Yamashina A *et al*. Validity, reproducibility, and clinical significance of noninvasive brachial-ankle pulse wave velocity measurement. *Hypertens Res* 2002; **25**: 359–364.
19 Munakata M, Ito N, Nunokawa T, Yoshinaga K. Utility of automated brachial ankle pulse wave velocity measurements in hypertensive patients. *Am J Hypertens* 2003; **16**: 653–657.
20 Yamashina A *et al*. Nomogram of the relation of brachial–ankle pulse wave velocity with blood pressure. *Hypertens Res* 2003; **26**: 801–806.

21 Yamashina A *et al.* Brachial–ankle pulse wave velocity as a marker of atherosclerotic vascular damage and cardiovascular risk. *Hypertens Res* 2003; **26**: 615–622.
22 Asmar R *et al.* Pulse pressure and aortic pulse wave are markers of cardiovascular risk in hypertensive populations. *Am J Hypertens* 2001; **14**: 91–97.
23 Guerin AP *et al.* Impact of aortic stiffness attenuation on survival of patients in end-stage renal failure. *Circulation* 2001; **103**: 987–992.
24 Peters MJ, Heyderman RS, Hatch DJ, Klein NJ. Investigation of platelet–neutrophil interactions in whole blood by flow cytometry. *J Immunol Methods* 1997; **209**: 125–135.
25 Hirai T, Sasayama S, Kawasaki T, Yagi S. Stiffness of systemic arteries in patients with myocardial infarction. A noninvasive method to predict severity of coronary atherosclerosis. *Circulation* 1989; **80**: 78–86.
26 Popele NM *et al.* Association between arterial stiffness and atherosclerosis: the Rotterdam Study. *Stroke* 2001; **32**: 454–460.
27 Blann AD, Lip GY, Beevers DG, McCollum CN. Soluble P-selectin in atherosclerosis: a comparison with endothelial cell and platelet markers. *Thromb Haemost* 1997; **77**: 1077–1080.
28 Bonfanti R, Furie BC, Furie B, Wagner DD. PADGEM (GMP140) is a component of Weibel–Palade bodies of human endothelial cells. *Blood* 1989; **73**: 1109–1112.
29 Hebert PR, Hennekens CH. An overview of the 4 randomized trials of aspirin therapy in the primary prevention of vascular disease. *Arch Intern Med* 2000; **160**: 3123–3127.
30 Goto S *et al.* Effects of ticlopidine on von Willebrand factor-mediated shear-induced platelet activation and aggregation. *Platelets* 2001; **12**: 406–414.
31 Nichols WW, O'Rourke MF. Effect of age and of hypertension on wave travel and reflections. *Arterial Vasodilation: Mechanisms and Therapy.* Arnold: London, 1993.
32 Kobayashi K *et al.* Interrelationship between non-invasive measurements of atherosclerosis: flow-mediated dilation of brachial artery, carotid intima-media thickness and pulse wave velocity. *Atherosclerosis* 2004; **173**: 13–18.
33 Dzau VJ, Gibbons GH. Vascular remodeling: mechanisms and implications. *J Cardiovasc Pharmacol* 1993; **21**: S1–S5.